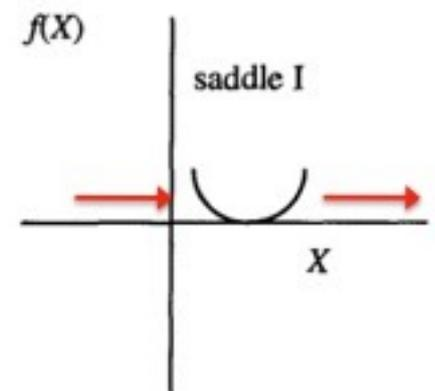
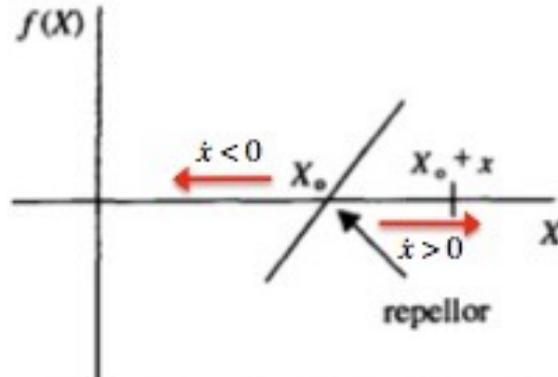
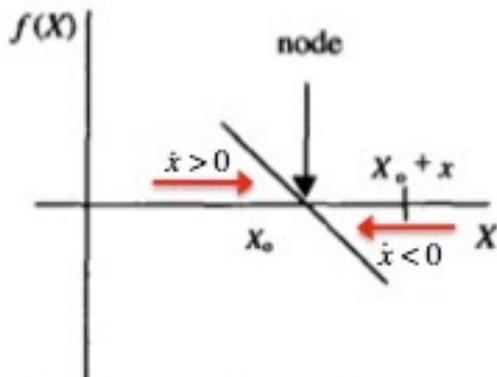


Flussi dissipativi in una dimensione

$$\frac{1}{L} \frac{dL}{dt} = \frac{1}{L} [f(X_B) - f(X_A)] = \frac{df(X)}{dX} < 0$$

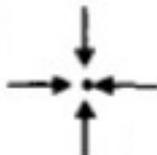
fixed points (dim.0)



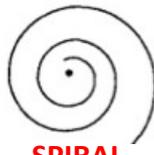
Flussi dissipativi in due dimensioni

$$\frac{1}{A} \frac{dA}{dt} = \frac{\partial f_1}{\partial X_1} + \frac{\partial f_2}{\partial X_2} < 0$$

fixed points (dim.0)



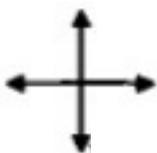
NODE



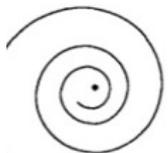
SPIRAL
NODE



SADDLE
POINTS

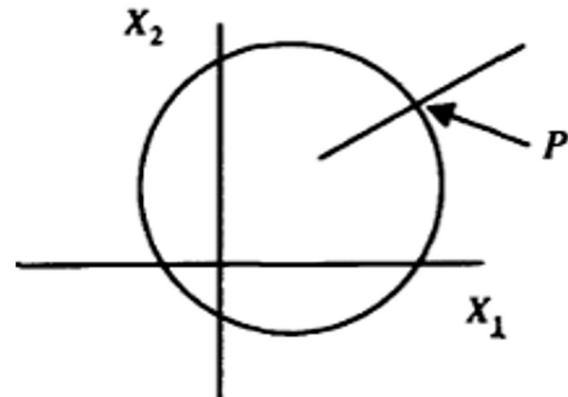


REPELLOR



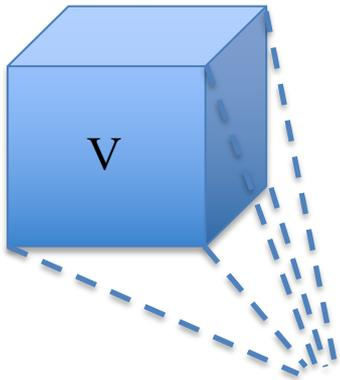
SPIRAL
REPELLOR

limit cycles (dim.1)



Flussi dissipativi in tre dimensioni

Cluster di
condizioni iniziali



ATTRATTORI

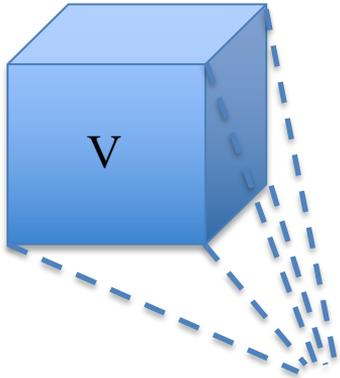
$$\frac{1}{V} \frac{dV}{dt} = \sum_{i=1}^N \frac{\partial f_i}{\partial x_i} \equiv \text{div}(f) < 0$$

fixed points (dim.0)

$$\begin{cases} \dot{x}_1 = f_1(x_1, x_2, x_3) \\ \dot{x}_2 = f_2(x_1, x_2, x_3) \\ \dot{x}_3 = f_3(x_1, x_2, x_3) \end{cases}$$

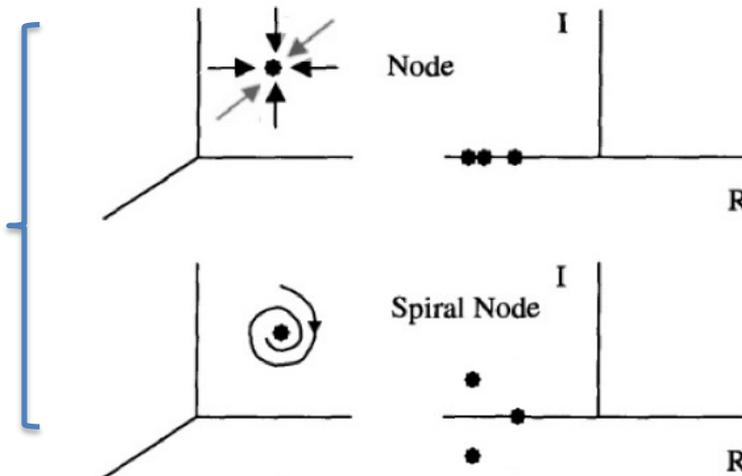
Flussi dissipativi in tre dimensioni

Cluster di
condizioni iniziali



ATTRATTORI

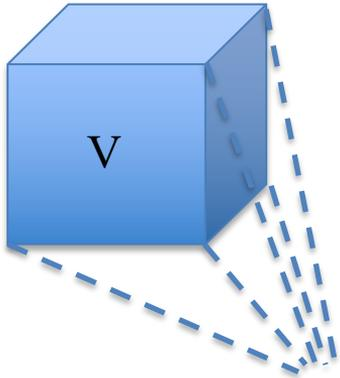
$$\frac{1}{V} \frac{dV}{dt} = \sum_{i=1}^N \frac{\partial f_i}{\partial x_i} \equiv \text{div}(f) < 0$$



$$J = \begin{pmatrix} \frac{\partial f_1}{\partial x_1} & \frac{\partial f_1}{\partial x_2} & \frac{\partial f_1}{\partial x_3} \\ \frac{\partial f_2}{\partial x_1} & \frac{\partial f_2}{\partial x_2} & \frac{\partial f_2}{\partial x_3} \\ \frac{\partial f_3}{\partial x_1} & \frac{\partial f_3}{\partial x_2} & \frac{\partial f_3}{\partial x_3} \end{pmatrix}$$

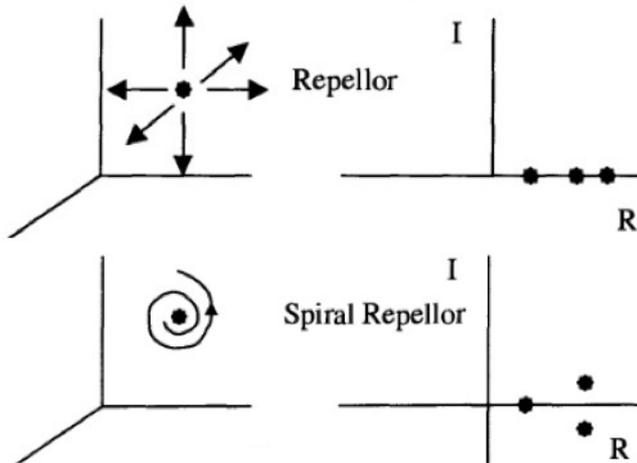
Flussi dissipativi in tre dimensioni

Cluster di
condizioni iniziali



ATTRATTORI

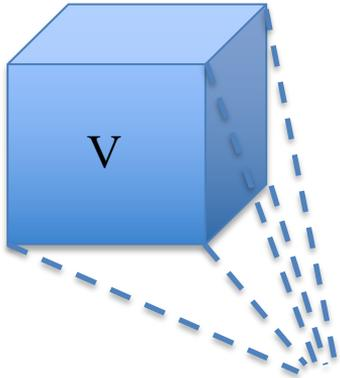
$$\frac{1}{V} \frac{dV}{dt} = \sum_{i=1}^N \frac{\partial f_i}{\partial x_i} \equiv \text{div}(f) < 0$$



$$J = \begin{pmatrix} \frac{\partial f_1}{\partial x_1} & \frac{\partial f_1}{\partial x_2} & \frac{\partial f_1}{\partial x_3} \\ \frac{\partial f_2}{\partial x_1} & \frac{\partial f_2}{\partial x_2} & \frac{\partial f_2}{\partial x_3} \\ \frac{\partial f_3}{\partial x_1} & \frac{\partial f_3}{\partial x_2} & \frac{\partial f_3}{\partial x_3} \end{pmatrix}$$

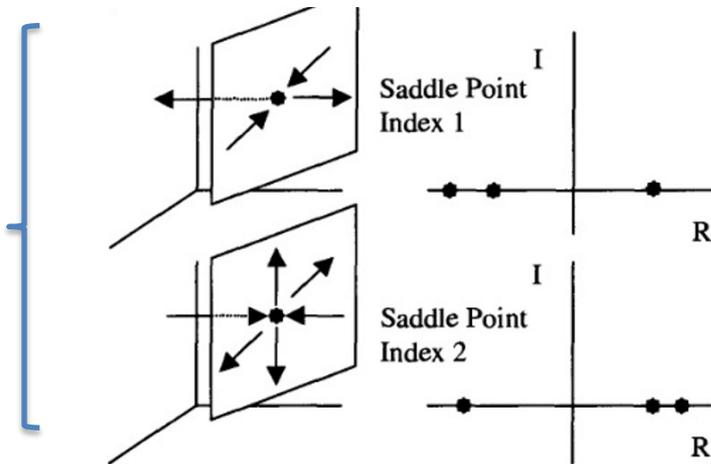
Flussi dissipativi in tre dimensioni

Cluster di
condizioni iniziali



ATTRATTORI

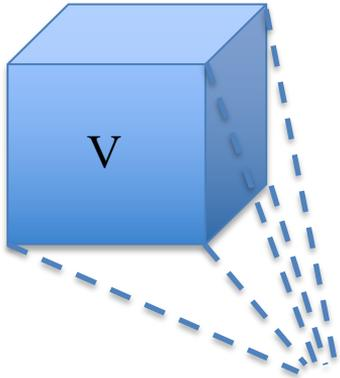
$$\frac{1}{V} \frac{dV}{dt} = \sum_{i=1}^N \frac{\partial f_i}{\partial x_i} \equiv \text{div}(f) < 0$$



$$J = \begin{pmatrix} \frac{\partial f_1}{\partial x_1} & \frac{\partial f_1}{\partial x_2} & \frac{\partial f_1}{\partial x_3} \\ \frac{\partial f_2}{\partial x_1} & \frac{\partial f_2}{\partial x_2} & \frac{\partial f_2}{\partial x_3} \\ \frac{\partial f_3}{\partial x_1} & \frac{\partial f_3}{\partial x_2} & \frac{\partial f_3}{\partial x_3} \end{pmatrix}$$

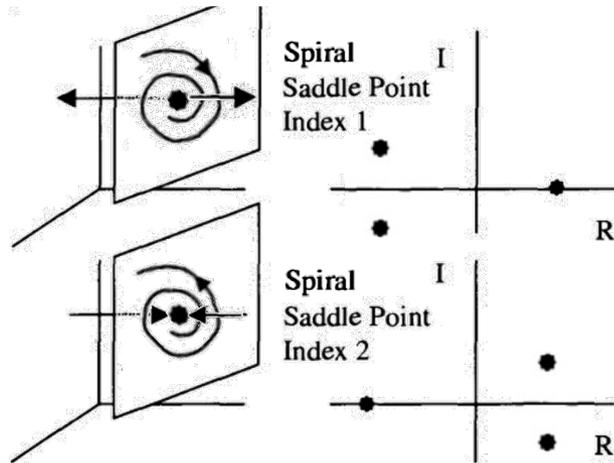
Flussi dissipativi in tre dimensioni

Cluster di
condizioni iniziali



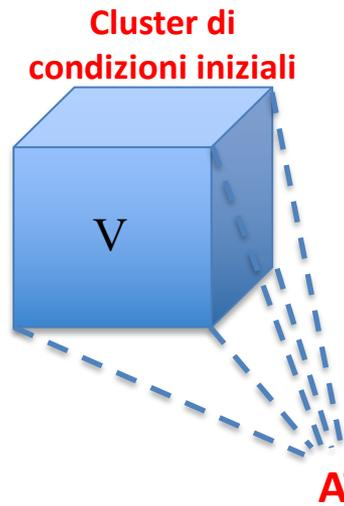
ATTRATTORI

$$\frac{1}{V} \frac{dV}{dt} = \sum_{i=1}^N \frac{\partial f_i}{\partial x_i} \equiv \text{div}(f) < 0$$



$$J = \begin{pmatrix} \frac{\partial f_1}{\partial x_1} & \frac{\partial f_1}{\partial x_2} & \frac{\partial f_1}{\partial x_3} \\ \frac{\partial f_2}{\partial x_1} & \frac{\partial f_2}{\partial x_2} & \frac{\partial f_2}{\partial x_3} \\ \frac{\partial f_3}{\partial x_1} & \frac{\partial f_3}{\partial x_2} & \frac{\partial f_3}{\partial x_3} \end{pmatrix}$$

Flussi dissipativi in tre dimensioni



$$\frac{1}{V} \frac{dV}{dt} = \sum_{i=1}^N \frac{\partial f_i}{\partial x_i} \equiv \text{div}(f) < 0$$

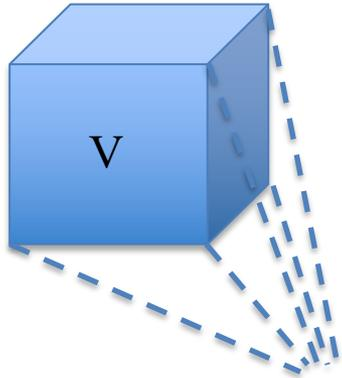
fixed points (dim.0)

limit cycles (dim.1)

$$\begin{cases} \dot{x}_1 = f_1(x_1, x_2, x_3) \\ \dot{x}_2 = f_2(x_1, x_2, x_3) \\ \dot{x}_3 = f_3(x_1, x_2, x_3) \end{cases}$$

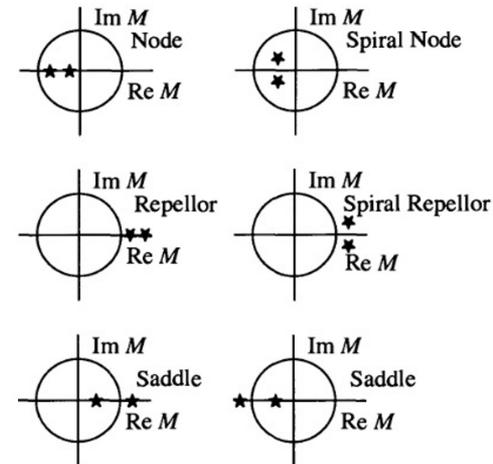
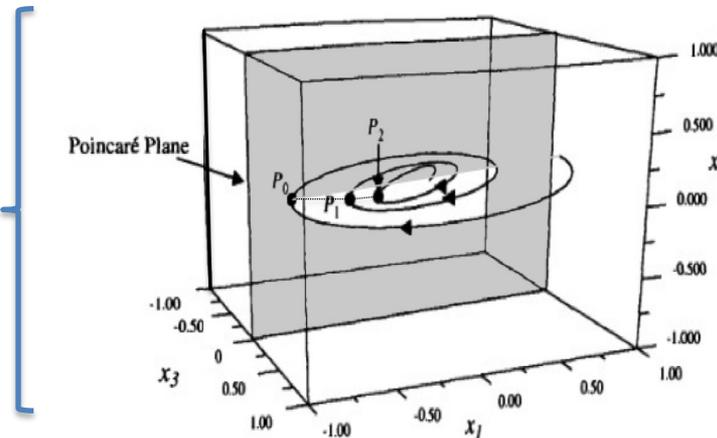
Flussi dissipativi in tre dimensioni

Cluster di
condizioni iniziali



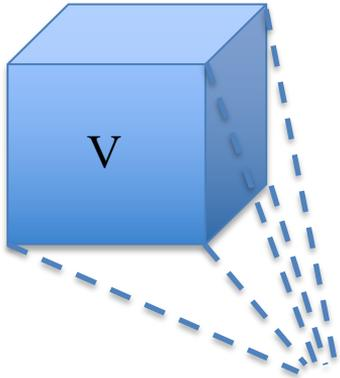
ATTRATTORI

$$\frac{1}{V} \frac{dV}{dt} = \sum_{i=1}^N \frac{\partial f_i}{\partial x_i} \equiv \text{div}(f) < 0$$



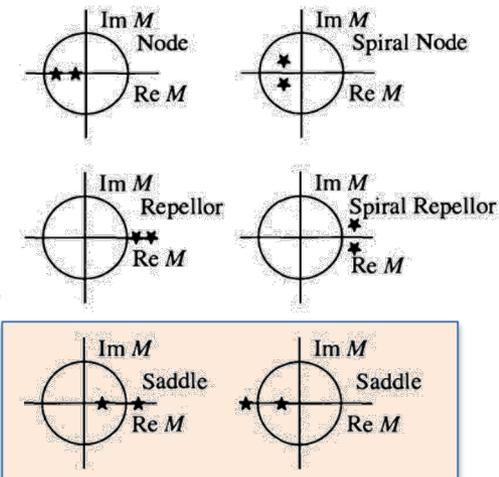
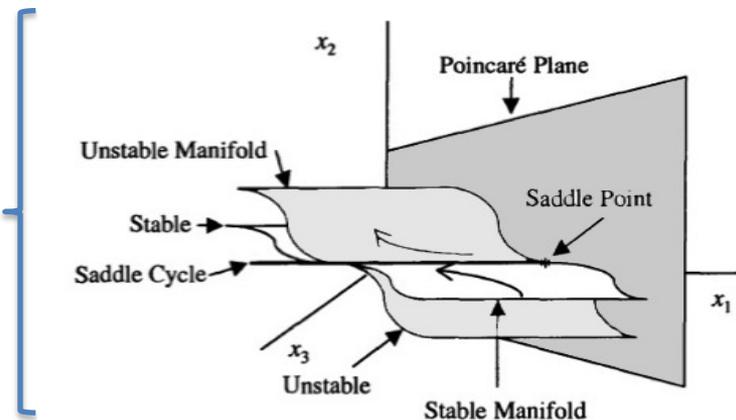
Flussi dissipativi in tre dimensioni

Cluster di
condizioni iniziali



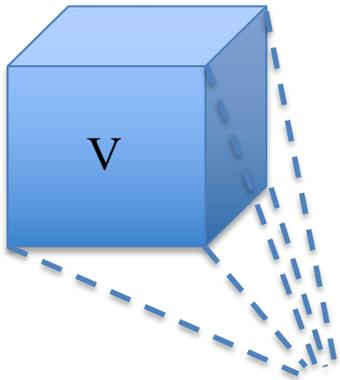
ATTRATTORI

$$\frac{1}{V} \frac{dV}{dt} = \sum_{i=1}^N \frac{\partial f_i}{\partial x_i} \equiv \text{div}(f) < 0$$



Flussi dissipativi in tre dimensioni

Cluster di
condizioni iniziali



ATTRATTORI

$$\frac{1}{V} \frac{dV}{dt} = \sum_{i=1}^N \frac{\partial f_i}{\partial x_i} \equiv \text{div}(f) < 0$$

fixed points (dim.0)

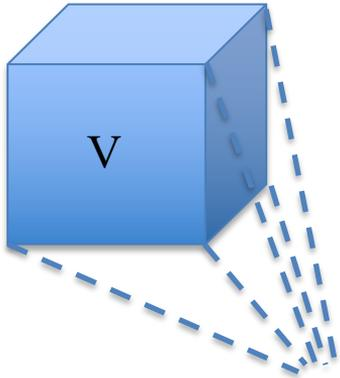
limit cycles (dim.1)

quasiperiodic attractors (dim.2)

$$\begin{cases} \dot{x}_1 = f_1(x_1, x_2, x_3) \\ \dot{x}_2 = f_2(x_1, x_2, x_3) \\ \dot{x}_3 = f_3(x_1, x_2, x_3) \end{cases}$$

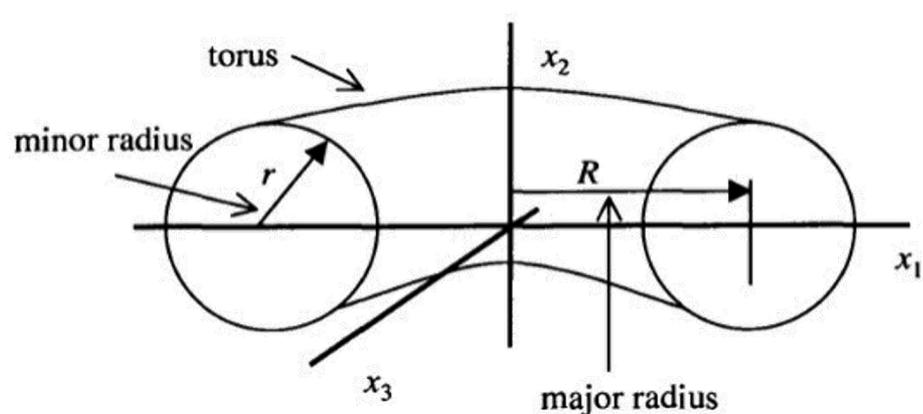
Flussi dissipativi in tre dimensioni

Cluster di
condizioni iniziali



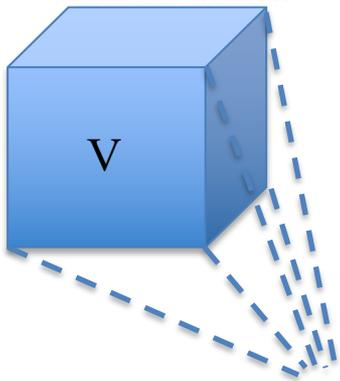
ATTRATTORI

$$\frac{1}{V} \frac{dV}{dt} = \sum_{i=1}^N \frac{\partial f_i}{\partial x_i} \equiv \text{div}(f) < 0$$



Flussi dissipativi in tre dimensioni

Cluster di
condizioni iniziali



ATTRATTORI

$$\frac{1}{V} \frac{dV}{dt} = \sum_{i=1}^N \frac{\partial f_i}{\partial x_i} \equiv \text{div}(f) < 0$$

fixed points (dim.0)

limit cycles (dim.1)

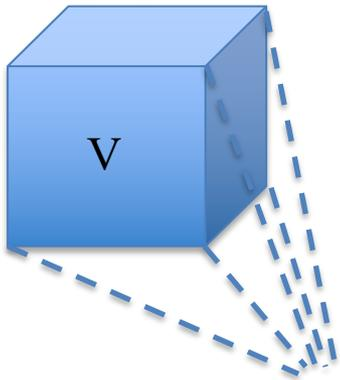
quasiperiodic attractors (dim.2)

chaotic attractors (fractal dimension between 2 and 3)

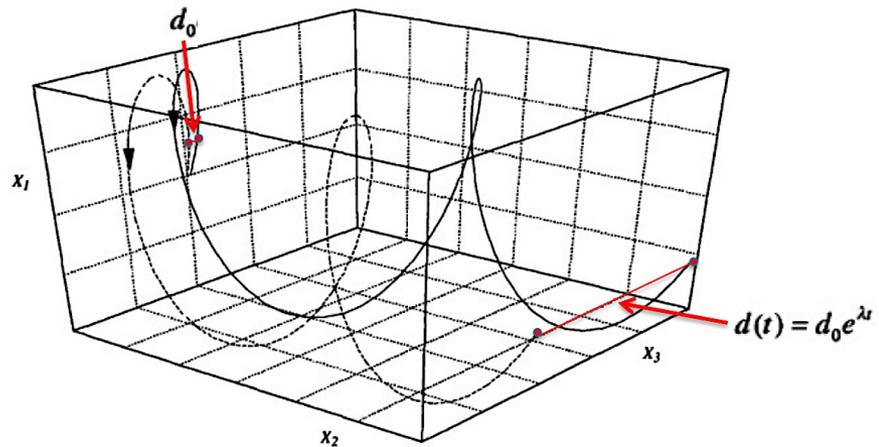
$$\begin{cases} \dot{x}_1 = f_1(x_1, x_2, x_3) \\ \dot{x}_2 = f_2(x_1, x_2, x_3) \\ \dot{x}_3 = f_3(x_1, x_2, x_3) \end{cases}$$

Flussi dissipativi in tre dimensioni

Cluster di
condizioni iniziali



ATTRATTORI

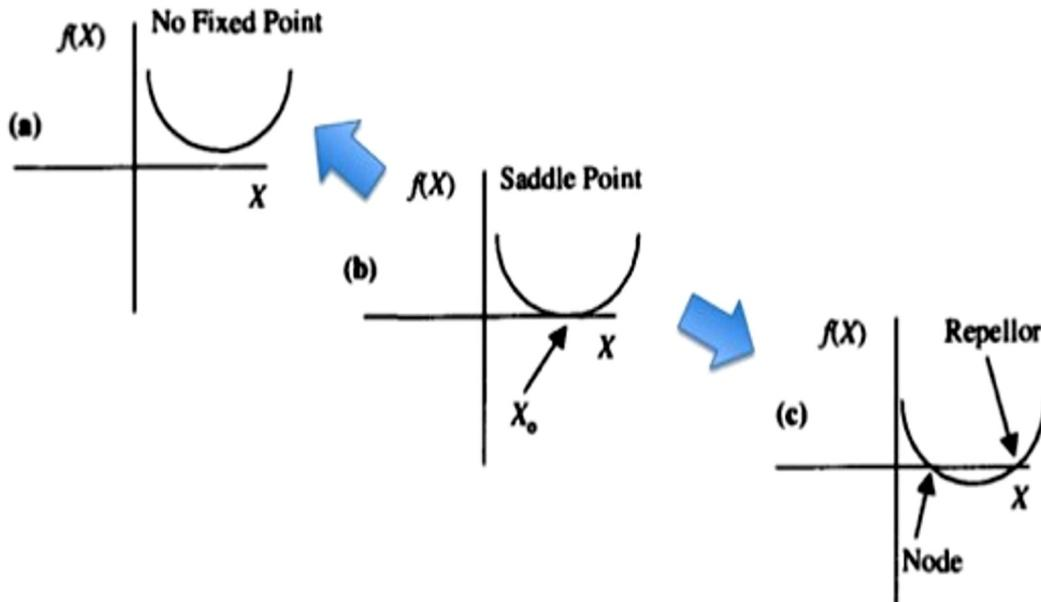


1. no intersection of different trajectories;
2. bounded trajectories;
3. exponential divergence of nearby trajectories.

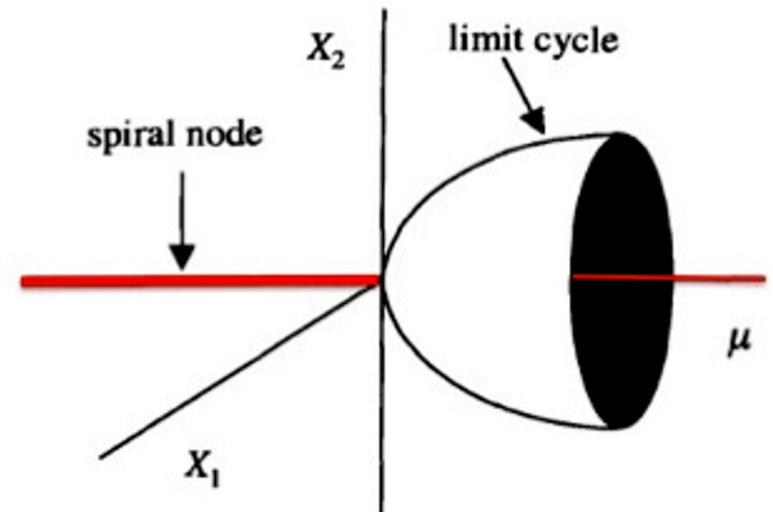
chaotic attractors (fractal dimension between 2 and 3)

Biforcazioni

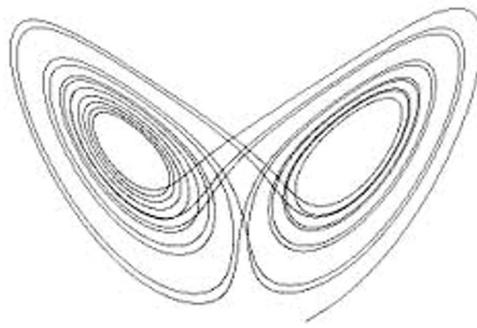
1D-2D: Repellor-Node (or Saddle-Node or Tangent) Bifurcation



2D: Hopf Bifurcation

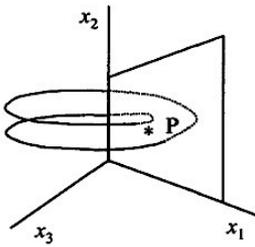
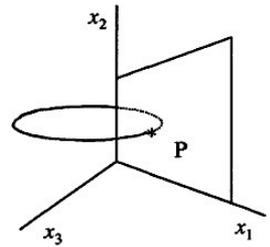


3D: . . . (Rotte verso il Caos...)

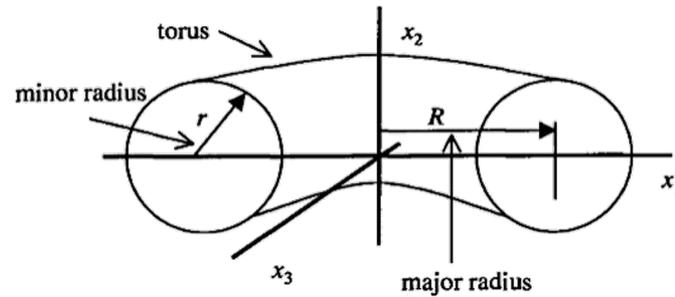


Rotte verso il CAOS...

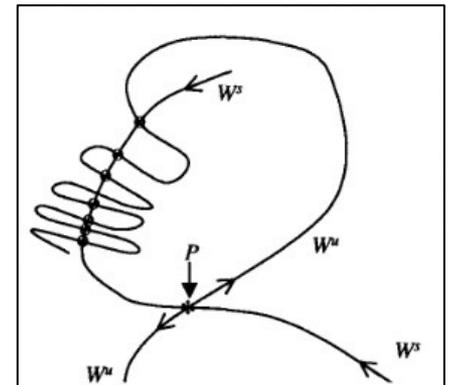
I : Period-Doubling



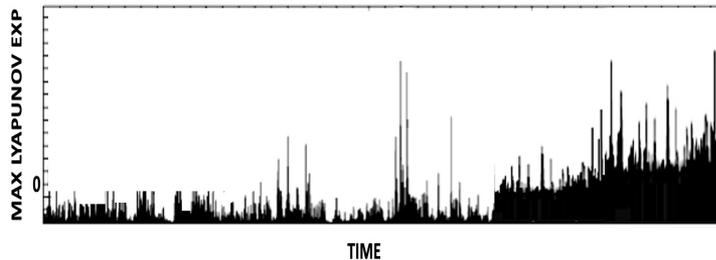
II : Quasi-Periodicity

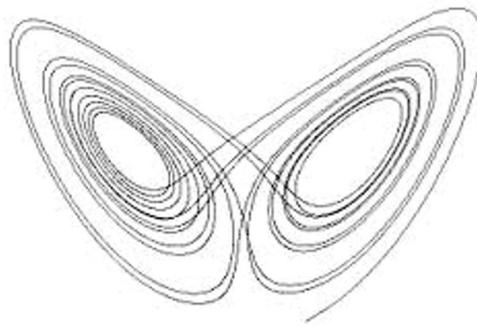


IV : Chaotic Transient and Homoclinic Orbits



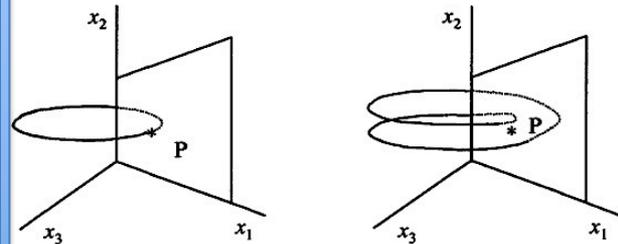
III : Intermittency and Crises





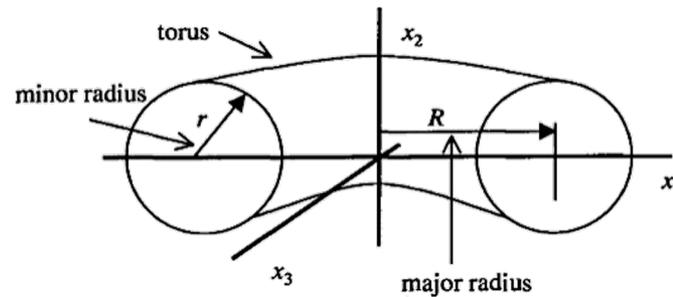
Rotte verso il CAOS...

I : Period-Doubling

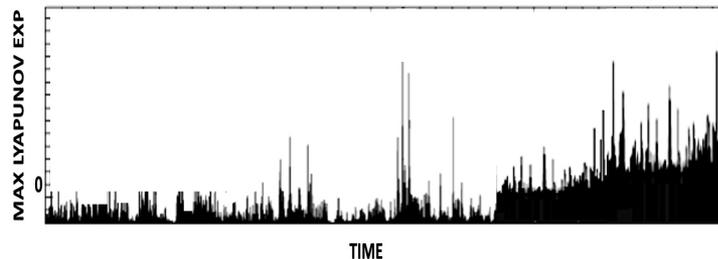


Local Bifurcations

II : Quasi-Periodicity

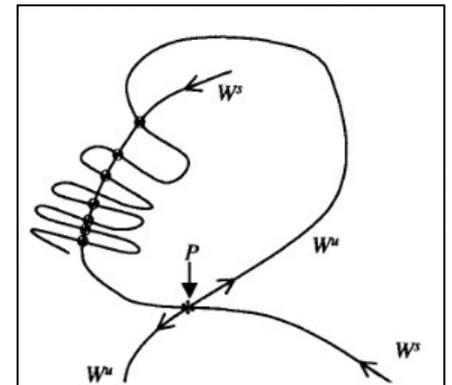


III : Intermittency and Crises



Global Bifurcations

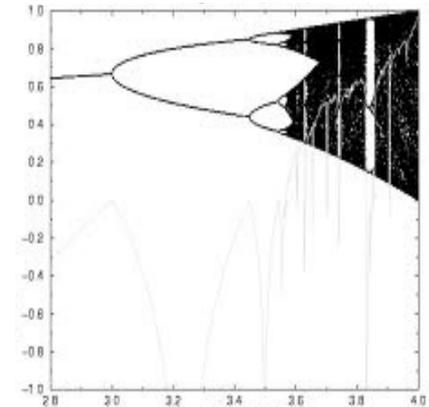
IV : Chaotic Transient and Homoclinic Orbits



Rotte verso il CAOS

When the parameters of a system are changed, chaotic behavior may appear and disappear in several different ways, even for the same dynamical system: We may have several routes to chaos. These routes can be put into two broad categories with several subdivisions within each category. One category includes sequences of bifurcations involving limit cycles (or equivalently, fixed points of the associated Poincaré map). (The period-doubling sequence in Chapter 1 belongs to this category.) The other category involves changes in trajectories associated with several fixed points or limit cycles. Since these changes involve the properties of trajectories ranging over a significant volume of state space, these changes are called “global” bifurcations (in contrast to “local” bifurcations associated with changes in individual fixed points).

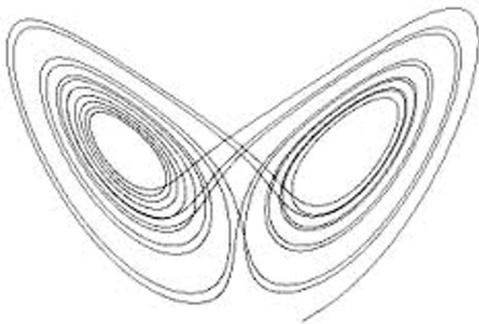
Local Bifurcations



Rather sudden changes from regular to chaotic behavior, such as we have seen with the Lorenz model in Chapter 1, are characteristic of these global bifurcations. Although the nature of the long-time attractor changes suddenly as a parameter is varied, these sudden changes are often heralded by chaotic transients. In a chaotic transient, the system's trajectory wanders through state space, in an apparently chaotic fashion. Eventually, the trajectory approaches a regular, periodic attractor. As the control parameter is changed, the chaotic transient lasts longer and longer until finally the asymptotic behavior is itself chaotic.

The questions we want to address are the following: How does this complicated chaotic behavior develop? How does the system evolve from regular, periodic behavior to chaotic behavior? What changes in the fixed points and in trajectories in state space give rise to these changes in behavior?

Global Bifurcations



I

4.8 The Routes to Chaos I: Period-Doubling

As we discussed earlier, the period-doubling route begins with limit cycle behavior of the system. This limit cycle, of course, may have been “born” from a bifurcation involving a node or other fixed point, but we need not worry about that now. As some control parameter changes, this limit cycle becomes unstable. Again this event is best viewed in the corresponding Poincaré section. Let us assume that the periodic limit cycle generates a single point in the Poincaré section. If the limit cycle becomes unstable by having one of its characteristic multipliers become more negative than -1 (which, of course, means $|M| > 1$), then, in many situations, the new motion remains periodic but has a period twice as long as the period of the original motion. In the Poincaré section, this new limit cycle exhibits two points, one on each side of the original Poincaré section point (see Fig. 4.10).

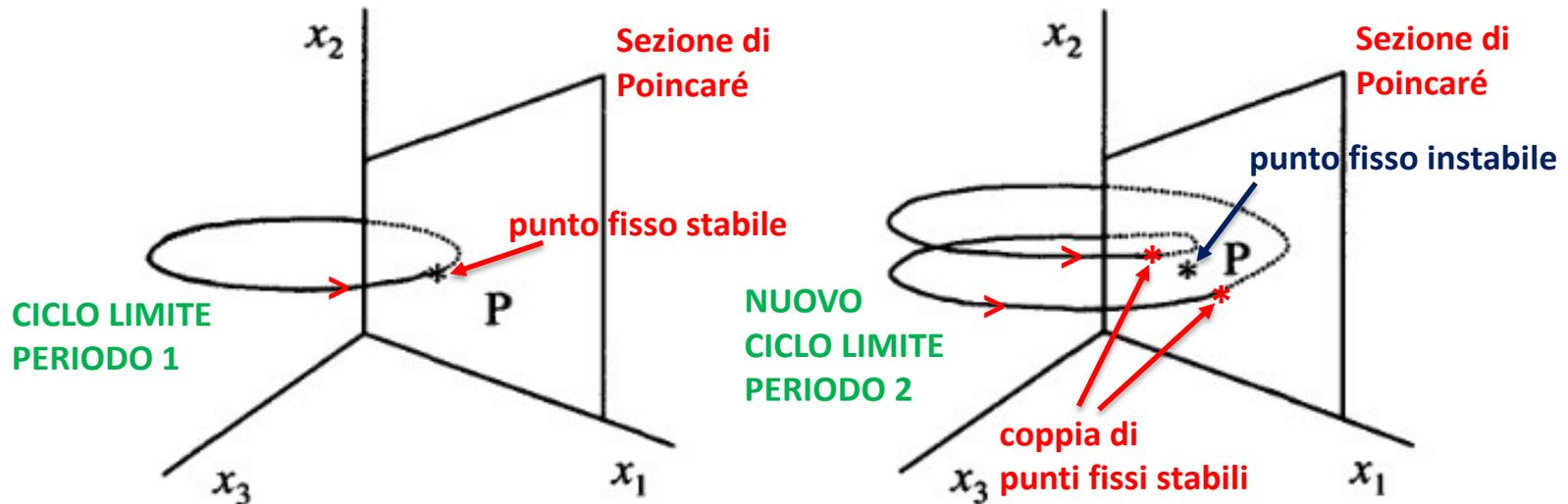
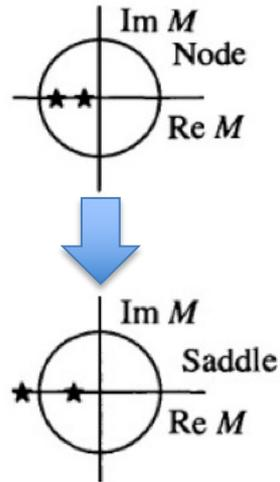
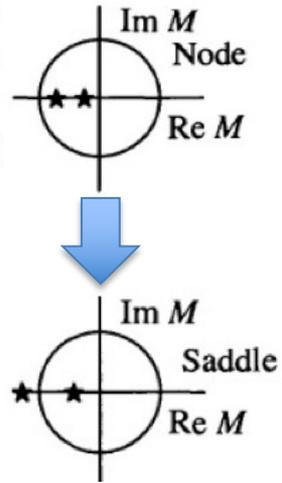


Fig. 4.10. The Poincaré section of a trajectory that has undergone a period-doubling bifurcation. On the left is the original periodic trajectory, which intersects the Poincaré plane in one point. On the right is the period-doubled trajectory, which intersects the Poincaré plane in two points, one on each side of the original intersection point.

This alternation of intersection points is related to the characteristic multiplier associated with the original limit cycle, which has gotten more negative than -1 . Since $|M| > 1$, the trajectory's map points are now being "repelled" by the original map point. The minus sign tells us that they alternate from one side to the other, as we can see formally from Eq. (3.16-6). This type of bifurcation is also called a flip bifurcation because the newly born trajectory flips back and forth from one side of the original trajectory to the other.

As the control parameter is changed further, this period-two limit cycle may become unstable and give birth to a period-four cycle with four Poincaré intersection points. Chapter 5 will examine in detail how, when, and where this sequence occurs. The period-doubling process may continue until the period becomes infinite; that is, the trajectory never repeats itself. The trajectory is then chaotic.



mappa 1 dim
 $d_{n+1} = M^n d_1$

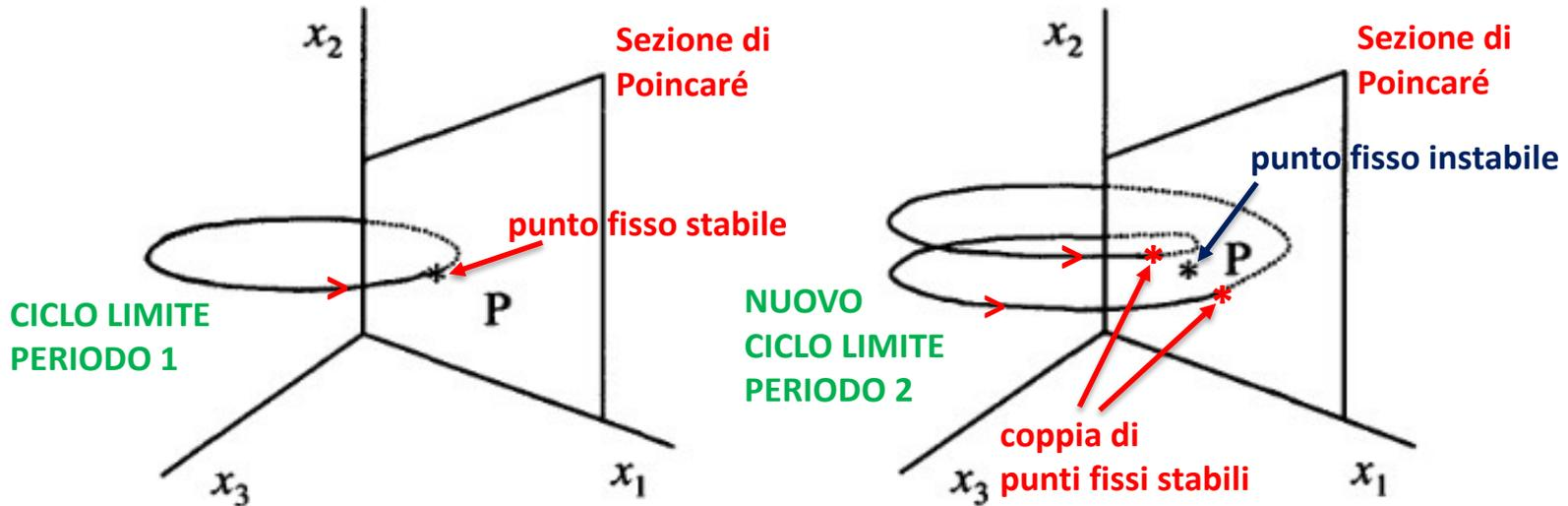


Fig. 4.10. The Poincaré section of a trajectory that has undergone a period-doubling bifurcation. On the left is the original periodic trajectory, which intersects the Poincaré plane in one point. On the right is the period-doubled trajectory, which intersects the Poincaré plane in two points, one on each side of the original intersection point.

II

4.9 The Routes to Chaos II: Quasi-Periodicity

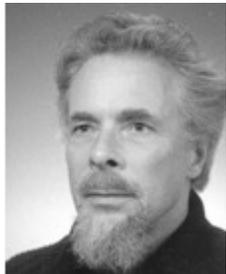
In the quasi-periodic scenario, the system begins again with a limit cycle trajectory. As a control parameter is changed, a second periodicity appears in the behavior of the system. This bifurcation event is a generalization of the Hopf bifurcation discussed in Chapter 3; so, it is also called a Hopf bifurcation. In terms of the characteristic multipliers, the Hopf bifurcation is marked by having the two complex-conjugate multipliers cross the unit circle simultaneously.

If the ratio of the period of the second type of motion to the period of the first is not a rational ratio, then we say, as described previously, that the motion is quasi-periodic. Under some circumstances, if the control parameter is changed further, the motion becomes chaotic. This route is sometimes called the Ruelle–Takens scenario after D. Ruelle and F. Takens, who in 1971 first suggested the theoretical possibility of this route. The main point here is that you might expect, at first thought, to see a long sequence of different frequencies come in as the control parameter is changed, much like the infinite sequence of period-doublings described in the previous section. (In 1944 the Russian physicist L. Landau had proposed such an infinite sequence of frequencies as a mechanism for producing fluid turbulence. [Landau and Lifshitz, 1959].) However, at least in some cases, the system becomes chaotic instead of introducing a third distinct frequency for its motion. This scenario will be discussed in Chapter 6.

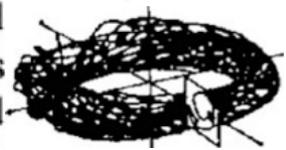
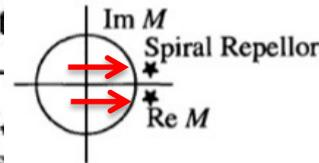
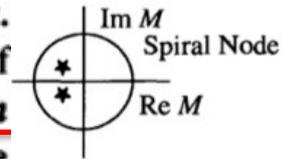
Historically, the experimental evidence for the quasi-periodic route to chaos (GOS75) played an important role in alerting the community of scientists to the utility of many of the newly emerging ideas in nonlinear dynamics. During the late 1970s and early 1980s there were many theoretical conjectures about the necessity of the transition from two-frequency quasi-periodic behavior to chaos. More recent work (see for example, BAT88) has shown that systems with significant spatial extent and with more degrees of freedom can have quasi-periodic behavior with three or more frequencies before becoming chaotic.



David Ruelle
(1935)



Floris Takens
(1940-2010)



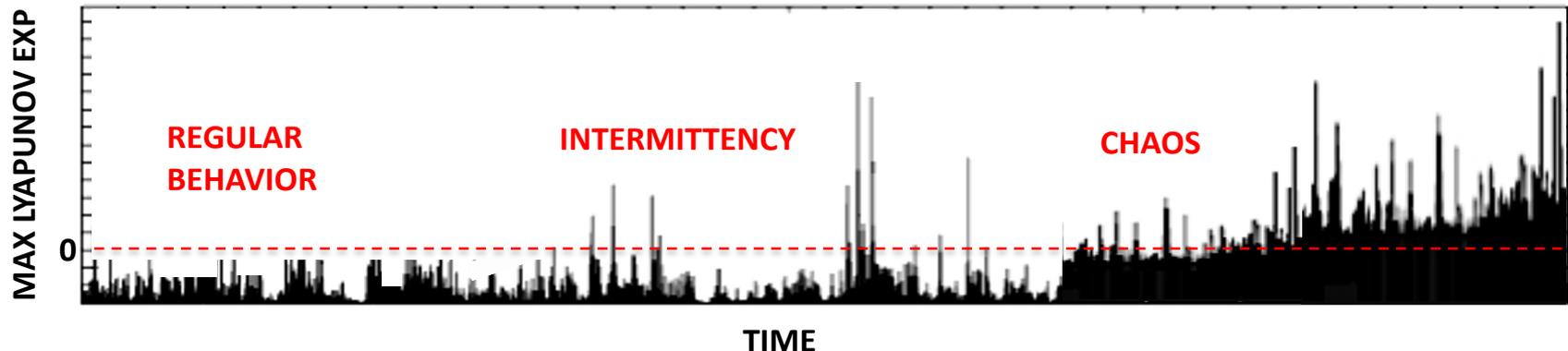
Lev Landau
(1908-1968)

III

4.10 The Routes to Chaos III: Intermittency and Crises

Chapter 7 contains a detailed discussion of intermittency and crises; so, we will give only the briefest description here. The **intermittency** route to chaos is characterized by dynamics with irregularly occurring bursts of chaotic behavior interspersed with intervals of apparently periodic behavior. As some control parameter of the system is changed, the chaotic bursts become longer and occur more frequently until, eventually, the entire time record is chaotic.

A **crisis** is a bifurcation event in which a chaotic attractor and its basin of attraction suddenly disappear or suddenly change in size as some control parameter is adjusted. Alternatively, if the parameter is changed in the opposite direction, the chaotic attractor can suddenly appear “out of the blue” or the size of the attractor can suddenly be reduced. As we shall see in Chapter 7, a crisis event involves the interaction between a chaotic attractor and an unstable fixed point or an unstable limit cycle.



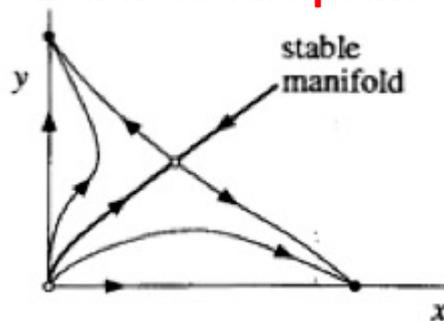
IV

4.11 The Routes to Chaos IV: Chaotic Transients and Homoclinic Orbits

In our second broad category of routes to chaos, the global bifurcation category, the chaotic transient route is the most important for systems modeled by sets of ordinary differential equations. Although the chaotic transient route to chaos was one of the first to be recognized in a model of a physical system (the Lorenz model), the theory of this scenario is, in some ways, less well developed than the theory for period-doubling, quasi-periodicity, and intermittency. This lack of development is due to the fact that this transition to chaos is not (usually) marked by any change in the fixed points of the system or the fixed points of a Poincaré section. The transition is due to the interaction of trajectories with various unstable fixed points and cycles in the state space. The common features are the so-called homoclinic orbits and their cousins, heteroclinic orbits. These special orbits may suddenly appear as a control parameter is changed. More importantly, these orbits strongly influence the nature of other trajectories passing near them.

What is a homoclinic orbit? To answer this question, we need to consider saddle cycles in a three-dimensional state space. (These ideas carry over in a straightforward fashion to higher-dimensional state spaces.) You should recall that saddle points and saddle cycles and, in particular, their in-sets and out-sets serve to organize the state space. That is, the in-sets and out-sets serve as “boundaries” between different parts of the state space and all trajectories must respect those boundaries. We will focus our attention on a saddle point in the Poincaré section of the state space. This saddle point corresponds to a saddle cycle in the original three-dimensional state space (see Fig. 4.11). We can consider the saddle cycle to be the intersection between two surfaces: One surface is the in-set (that is, the stable manifold) associated with the cycle. The other surface is the out-set (unstable manifold) associated with the cycle. Trajectories on the in-set approach the saddle cycle as time goes on. Trajectories on the out-set diverge from the cycle as time goes on. Trajectories that are near to, but not on, the in-set will first approach the cycle and then be repelled roughly along the out-set (unstable manifold).

2 dim: saddle point



3 dim: saddle cycle

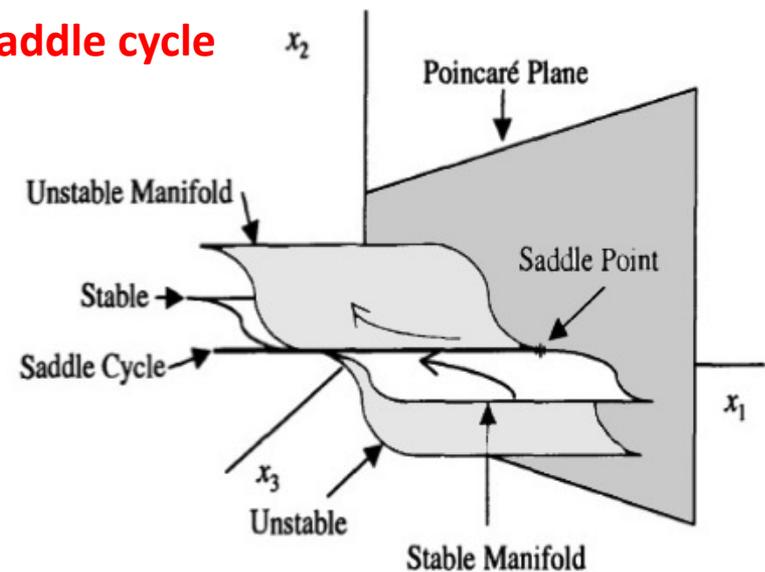


Fig. 4.11. A saddle cycle in a three-dimensional state space. The stable and unstable manifolds are surfaces that intersect at the saddle cycle. Where the saddle cycle intersects a Poincaré plane we have a saddle point for the Poincaré map function. A portion of one trajectory, repelled by the saddle cycle, is shown on the unstable manifold, and a portion of another trajectory, approaching the saddle cycle, is shown on the stable manifold.

Fig. 4.12 shows the equivalent Poincaré section with a saddle point P where the saddle cycle intersects the plane. We have sketched in some curves to indicate schematically where the in-set and out-set surfaces cut the Poincaré plane. These curves, labeled $W^s(P)$ and $W^u(P)$, are called the stable and unstable manifolds of the saddle point P . Since the in-set and out-set of a saddle cycle are generally two-dimensional surfaces (in the original three-dimensional state space), the intersection of one of these surfaces with the Poincaré plane forms a curve. It is crucial to realize that these curves are not trajectories. For example, if we pick a point s_0 on $W^s(P)$, a point at which some trajectory intersects the Poincaré plane, then the Poincaré map function F gives us s_1 , the coordinates of the point at which the trajectory next intersects the plane. From s_1 , we can find s_2 , and so on. The sequence of points lies along the curve labeled $W^s(P)$ and approaches P as $n \rightarrow \infty$. Similarly, if u_0 is a point along $W^u(P)$, then $F(u_0) = u_1$, $F(u_1) = u_2$, and so on, generates a series of points that diverges from P along $W^u(P)$. If we apply the inverse of the Poincaré map function $F^{(-1)}$ to u_0 , we generate a sequence of points u_{-1} , u_{-2} , and so on, that approaches P as $n \rightarrow -\infty$. The curves drawn in Fig. 4.12 represent the totality of such sequences of points taken with infinitely many starting points. For any one starting point, however, the sequence jumps along W^s or W^u , it does not move smoothly like a point on a trajectory in the original state space.

Sezione
di Poincarè

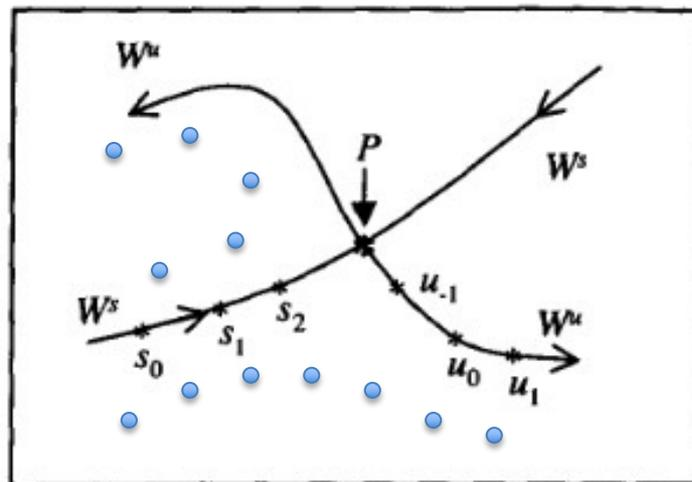


Fig. 4.12. Point P is a saddle point in a Poincaré section. It corresponds to a saddle cycle in the full three-dimensional state space. The intersection of the in-set of the saddle cycle with the Poincaré plane generates the curve labeled W^s . The intersection of the out-set of the saddle cycle with the Poincaré plane generates curve W^u .

As a control parameter is changed, it is possible for $W^s(P)$ and $W^u(P)$ to approach each other and in fact to intersect, say, at some point q . If this intersection occurs, we say that we have a homoclinic intersection at q , and the point q is called a homoclinic (intersection) point. It is also possible for the unstable manifold of one saddle point to intersect the stable manifold from some other saddle point. In that case we say we have a heteroclinic intersection. Other heteroclinic combinations are possible. For example, we could have the intersection of the unstable manifold surface of an index-2 saddle point and the stable manifold of a saddle cycle. (For a nice visual catalog of the possible kinds of intersections, see [Abraham and Shaw, 1992][Abraham, Abraham, and Shaw, 1996].) For now we will concentrate on homoclinic intersections.

We now come to an important and crucial theorem:

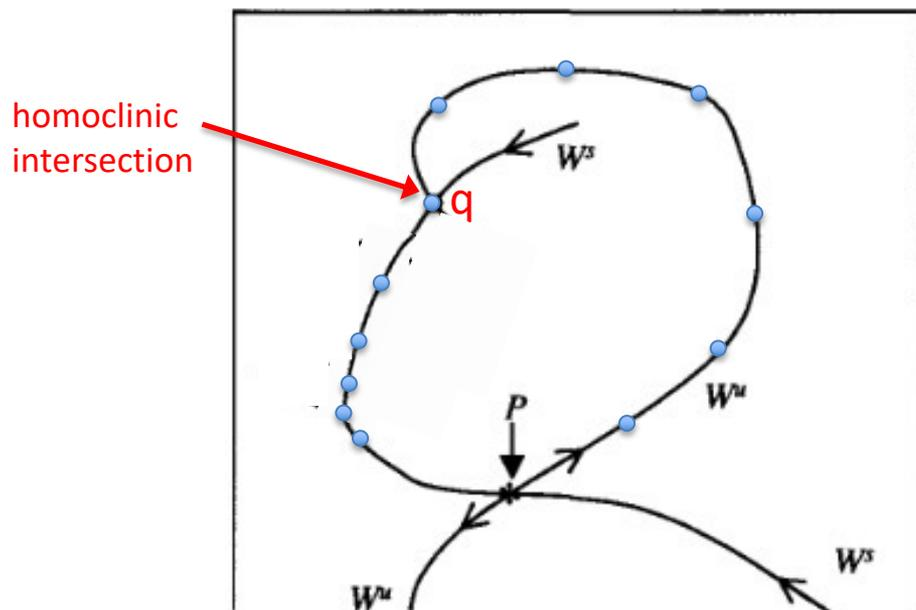


Fig. 4.13. A homoclinic tangle results from the homoclinic intersection of the unstable manifold $W^u(P)$ with the stable manifold $W^s(P)$ of the saddle point P . Each of the circled points is a homoclinic (intersection) point. For clarity's sake, only a portion of the tangle is shown.

TEOREMA

If the in-sets and out-sets of a saddle point in the Poincaré section of a dynamical system intersect at one homoclinic intersection point q_0 , then there must be an infinite number of homoclinic intersections.

To prove this statement, we consider the result of applying the mapping function F to q_0 . We get another point q_1 . Since q_0 belongs to both W^s and W^u , so must q_1 , since we have argued in the previous paragraphs that applying F to a point on W^s or W^u generates another point on W^s or W^u . By continuing to apply F to this sequence of points, we generate an infinite number of homoclinic points. Fig. 4.13 shows part of the resulting homoclinic tangle, which must result from the homoclinic intersections.

Please note that the smooth curves drawn in Fig. 4.13 are not individual trajectories. (We cannot violate the No-Intersection Theorem!) The smooth curves are generated by taking infinitely many starting points on W^s and W^u . Only those trajectories that hit one of the homoclinic points will hit (some of) the other homoclinic points.

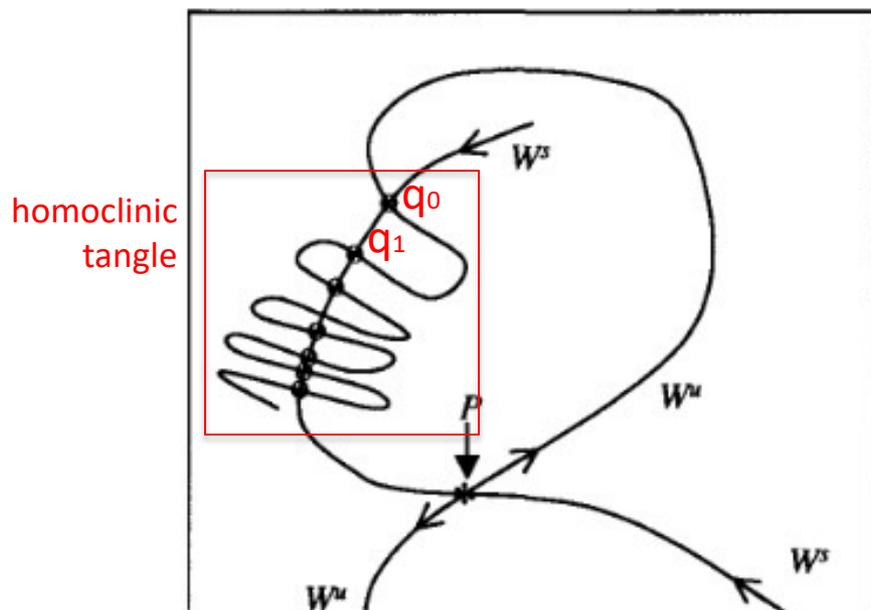
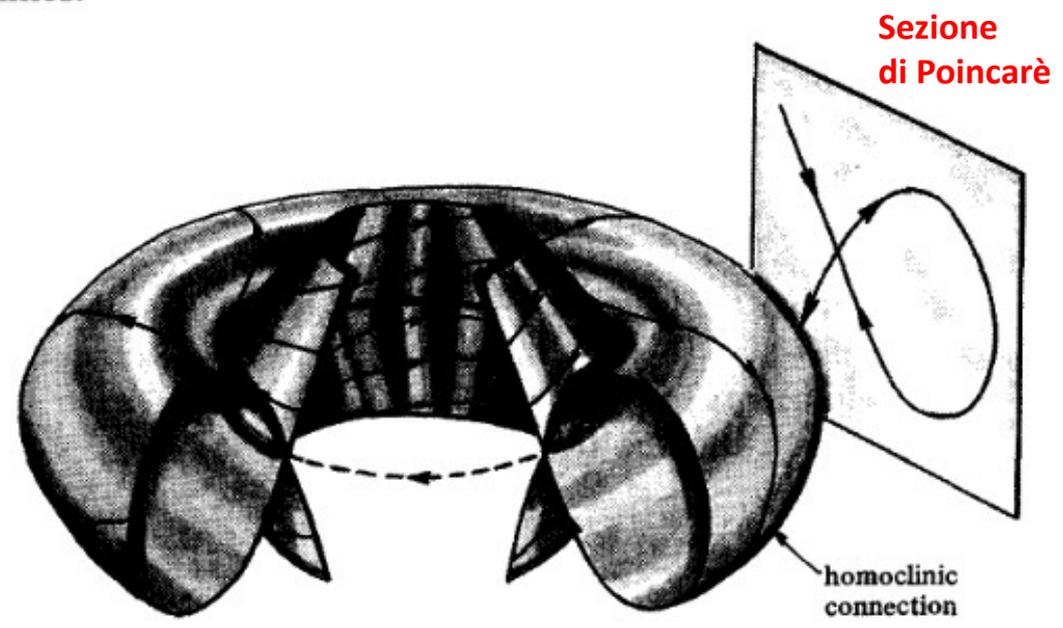
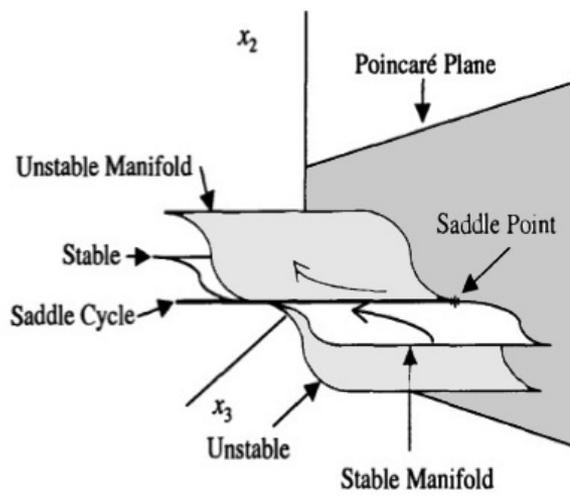


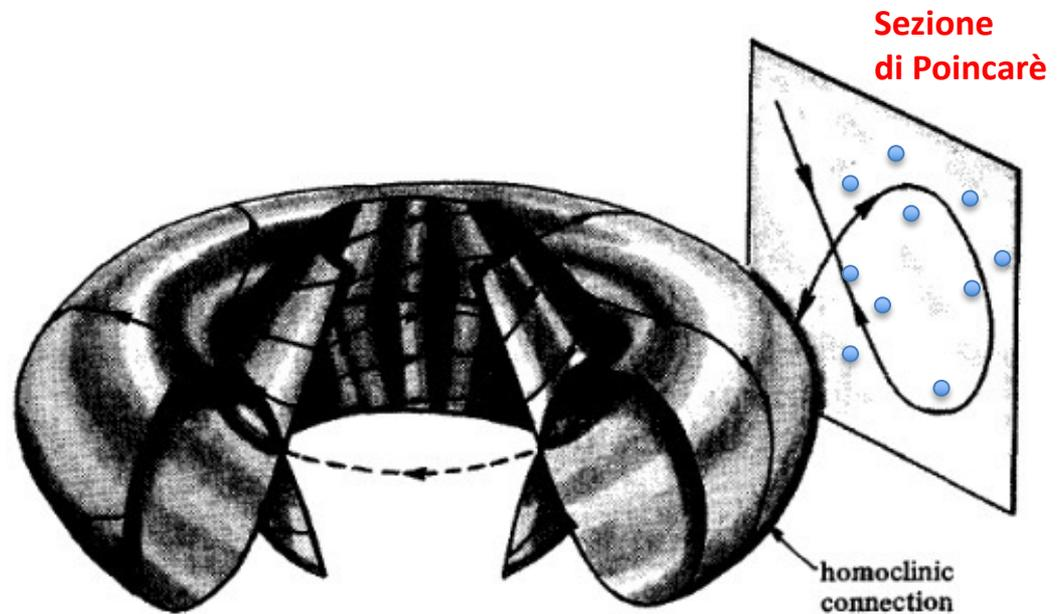
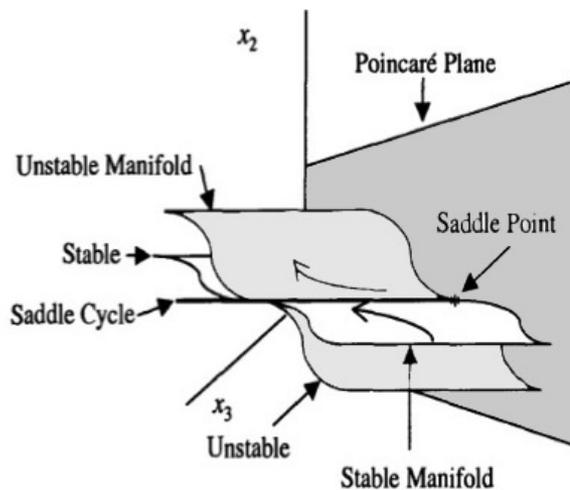
Fig. 4.13. A homoclinic tangle results from the homoclinic intersection of the unstable manifold $W^u(P)$ with the stable manifold $W^s(P)$ of the saddle point P . Each of the circled points is a homoclinic (intersection) point. For clarity's sake, only a portion of the tangle is shown.

What is the dynamical significance of a homoclinic point and the related homoclinic tangle? If we now shift our attention back to the original three-dimensional state space, we see that a homoclinic point in the Poincaré section corresponds to a continuous trajectory in the original state space. When a homoclinic intersection occurs, one trajectory on the unstable manifold joins another trajectory on the stable manifold to form a single new trajectory whose Poincaré intersection points are the homoclinic points described earlier. (To help visualize this process, recall that the in-set and out-set of a saddle cycle in the three-dimensional state space are, in general, two-dimensional surfaces.) This new trajectory connects the saddle point to itself and hence is called a homoclinic trajectory or homoclinic orbit and is said to form a homoclinic connection. As our previous theorem states, this homoclinic trajectory must intersect the Poincaré plane an infinite number of times.



(a)

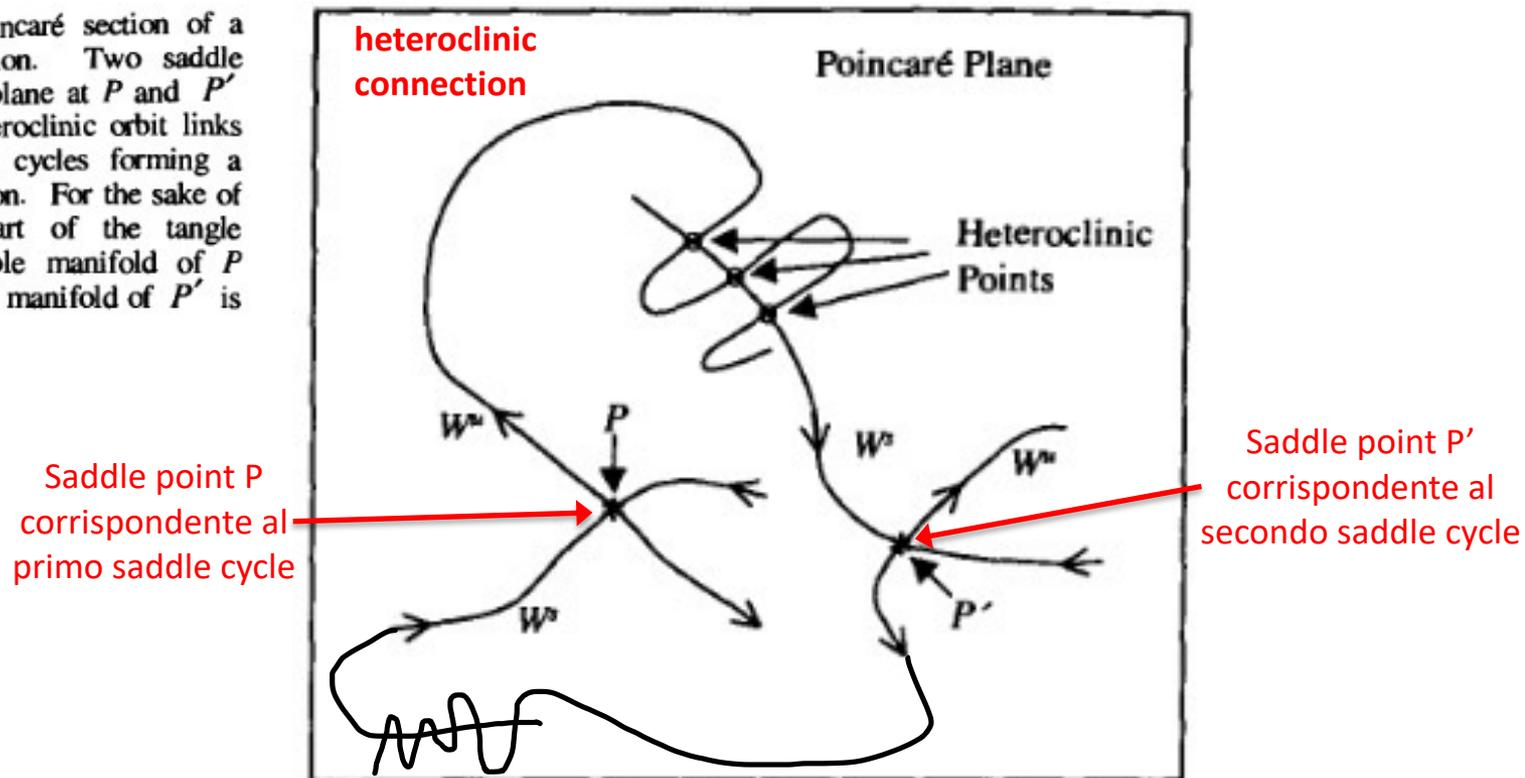
How does a homoclinic orbit lead to chaotic behavior? To understand this, we need to consider other trajectories that come near the saddle point of the Poincaré section. Generally speaking, the trajectories approach the saddle point close to (but not on) the in-set (stable manifold), but they are then forced away from the saddle point near the out-set (unstable manifold). After a homoclinic tangle has developed, a trajectory will be pushed away from the saddle point by the out-set part of the tangle, but it will be pulled back by the in-set part. It is easy to see that the homoclinic tangle can lead to trajectories that seem to wander randomly around the state space region near the saddle point.



(a)

The same general type of behavior can result from a heteroclinic orbit, which connects one saddle point (or saddle cycle in the original state space) to another. A second heteroclinic orbit takes us from the second saddle point back to the first. When such a combined trajectory exists, we say we have a heteroclinic connection between the two saddle cycles. Figure 4.14 shows schematically a part of a heteroclinic connection in a Poincaré section of a three-dimensional state space. It is also possible to have heteroclinic orbits that link together sequentially three or more saddle cycles.

Fig. 4.14. The Poincaré section of a heteroclinic connection. Two saddle cycles intersect the plane at P and P' respectively. A heteroclinic orbit links together two saddle cycles forming a heteroclinic connection. For the sake of clarity only the part of the tangle involving the unstable manifold of P intersecting the stable manifold of P' is shown



heteroclinic connections in three-dimensional state spaces for which the in-sets and out-sets of a saddle cycle are two-dimensional surfaces. Also shown are partial pictures of the resulting Poincaré sections.

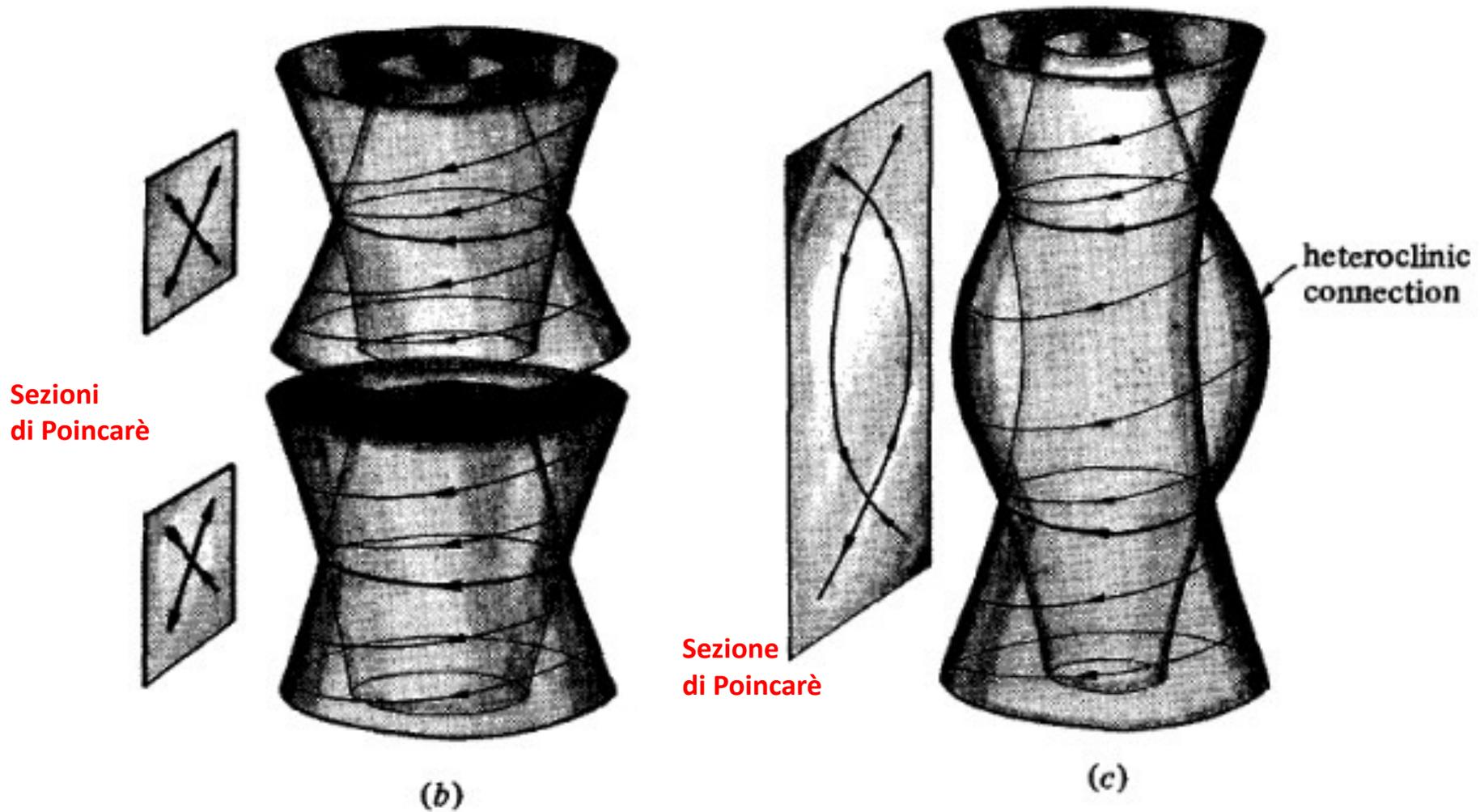
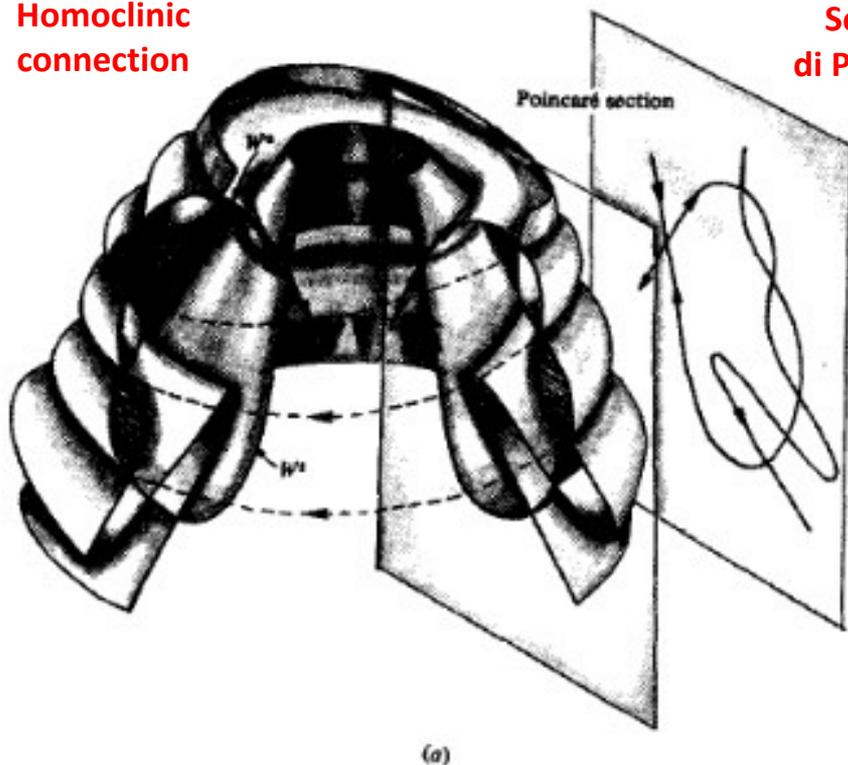
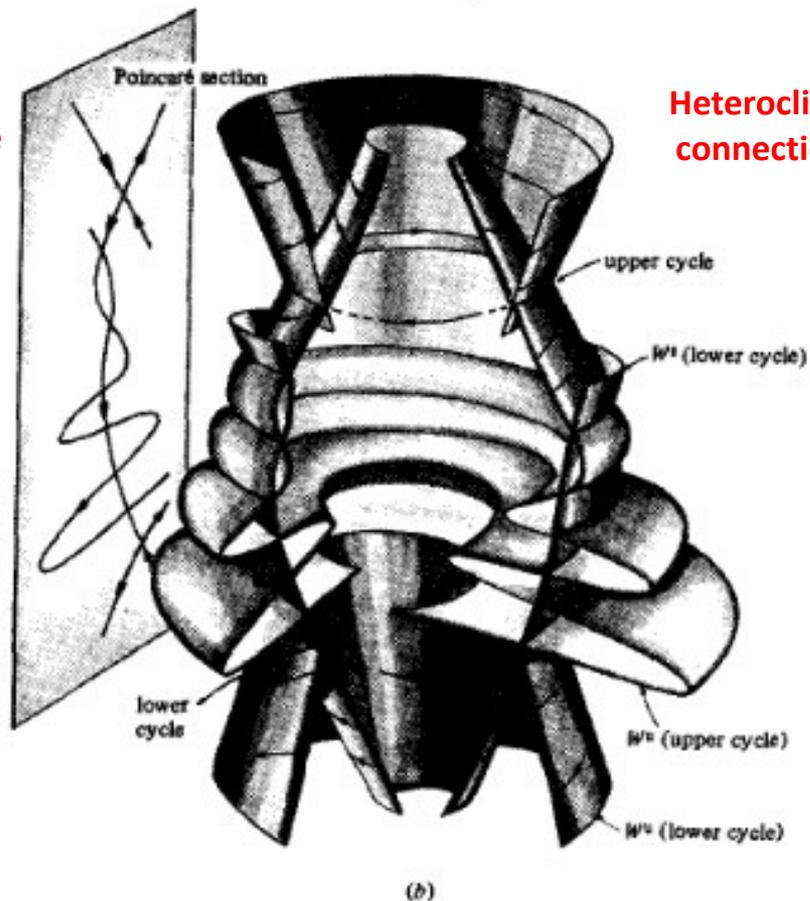


Figure 4.16 shows three-dimensional constructions of homoclinic and heteroclinic tangles resulting from the intersections of the in-sets and out-sets of saddle cycles. Partial diagrams of the corresponding Poincaré sections are also shown.

Homoclinic connection



Sezioni di Poincaré



Heteroclinic connection

Così, nel terzo volume del suo *Méthodes nouvelles de la mécanique céleste* (1882-1889), lo stesso Poincaré descrisse la scoperta del «tangle» omoclinico compiuta mentre cercava di risolvere il problema dei tre corpi per mezzo della sua «sezione» (non avendo all'epoca i computer, ovviamente non poté mai visualizzarla...):

«Tentiamo di farci un'idea della figura formata da queste due curve e delle loro intersezioni, che sono in numero infinito e corrispondono ciascuna a una soluzione doppiamente asintotica; queste intersezioni formano una sorta di reticolo, di ordito, di rete dalle maglie infinitamente fitte; ciascuna delle due curve non deve mai intersecare se stessa, ma deve ripiegarsi su se stessa in maniera assai complicata per poter intersecare un'infinità di volte tutte le maglie della rete».

Per approfondimenti: <https://www.vitapensata.eu/2022/01/04/tre-corpi-al-margine-del-caos/>

(Tre) corpi al margine del caos

Di: **Alessandro Pluchino**

4 Gennaio 2022

Come è noto, il Tre è spesso considerato il *numero perfetto* da diversi punti di vista: dal punto di vista *matematico* costituisce la sintesi dei pari (due) e del dispari (uno); dal punto di vista *esoterico* è il simbolo della Grande Triade (Cielo, Terra, Uomo); infine, dal punto di vista *religioso*, rappresenta la perfezione divina (si pensi alla Trinità del Cristianesimo o alla Trimurti induista). Pochi forse sanno, però, che allo stesso tempo il tre rappresenta anche la *soglia dell'imperfezione*, il numero magico che ha condotto la fisica moderna al confine tra ordine e disordine, in quella strana regione oggi conosciuta come "Margine del Caos", spalancando così le porte alla nuova Scienza della Complessità. E la scintilla da cui questa rivoluzione concettuale è partita riguardava un problema di corpi. Per la precisione, appunto, di tre corpi.

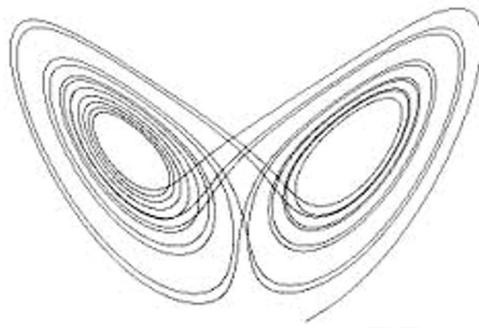


Tutto cominciò la notte tra il 31 agosto e il primo settembre del 1879 in una miniera di carbone di Magny, nella Borgogna francese. Alle 3.45 circa del mattino un'esplosione improvvisa scosse la miniera, ustionando e uccidendo gran parte della squadra di ventidue minatori che si trovavano al lavoro a quell'ora. Fu soltanto la perizia e l'acume scientifico di un giovane ingegnere incaricato delle indagini a permettere di risalire alla causa prima dell'esplosione: si era trattato di una lampada perforata accidentalmente che aveva lasciato uscire la fiamma da cui poi, a contatto con un'atmosfera ricca di metano come quella della miniera, aveva avuto inizio il processo che avrebbe portato alla conflagrazione. Quel giovane ingegnere, appena venticinquenne, si chiamava Jules-Henri Poincaré, colui che più avanti si sarebbe distinto come uno dei più grandi matematici e fisici di fine Ottocento (all'epoca si poteva essere ingegnere, matematico e fisico allo stesso tempo!) e che è considerato oggi uno dei padri della teoria dei sistemi dinamici e il precursore assoluto della moderna teoria del Caos. Sarà lui il principale protagonista della storia che stiamo per raccontarvi.

Così, nel terzo volume del suo *Méthodes nouvelles de la mécanique céleste* (1882-1889), lo stesso Poincaré descrisse la scoperta del «tangle» omoclinico compiuta mentre cercava di risolvere il problema dei tre corpi per mezzo della sua «sezione» (non avendo all'epoca i computer, ovviamente non poté mai visualizzarla...):

«Tentiamo di farci un'idea della figura formata da queste due curve e delle loro intersezioni, che sono in numero infinito e corrispondono ciascuna a una soluzione doppiamente asintotica; queste intersezioni formano una sorta di reticolo, di ordito, di rete dalle maglie infinitamente fitte; ciascuna delle due curve non deve mai intersecare se stessa, ma deve ripiegarsi su se stessa in maniera assai complicata per poter intersecare un'infinità di volte tutte le maglie della rete».





Rotte verso il CAOS...

IL MODELLO DI LORENZ



The Lorenz Equations

The Lorenz model is based on a (gross) simplification of the fundamental Navier-Stokes equations for fluids. As shown in Appendix C, the fluid motion and resulting temperature differences can be expressed in terms of three variables, conventionally called $X(t)$, $Y(t)$, and $Z(t)$.



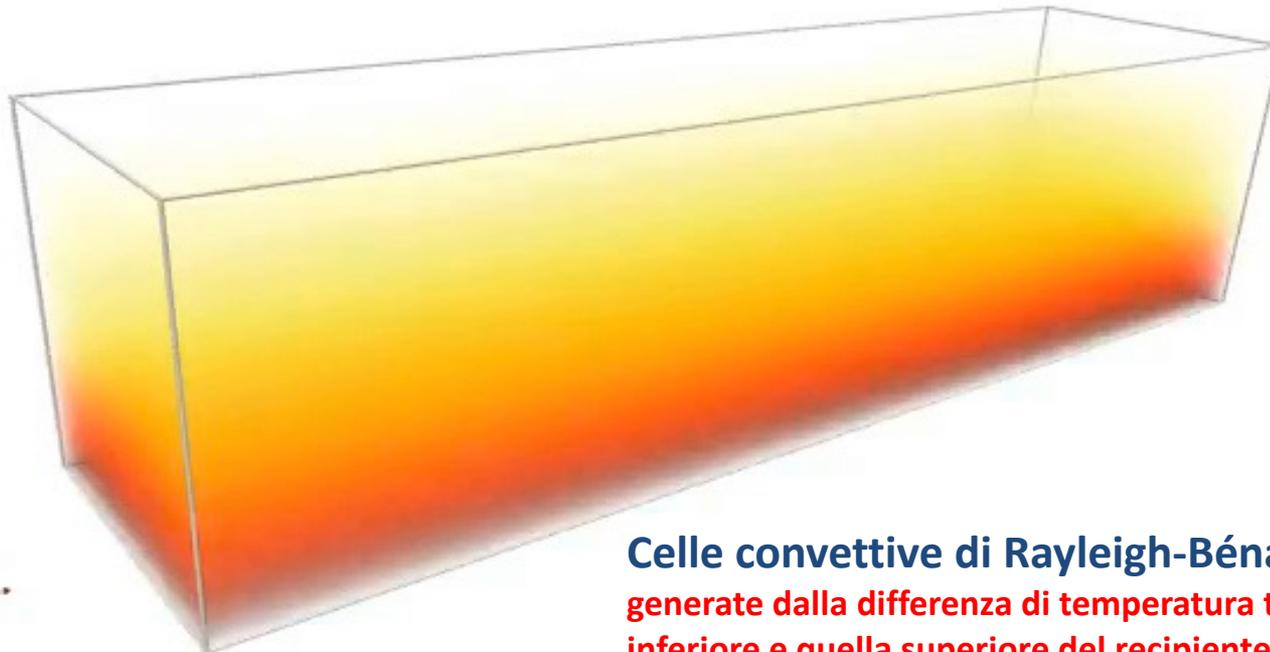
$$\begin{cases} \dot{X} = p(Y - X) \\ \dot{Y} = -XZ + rX - Y \\ \dot{Z} = XY - bZ \end{cases}$$

Significato delle 3 variabili:

$X(t)$: dipendenza temporale della funzione di flusso del fluido (le cui derivate rispetto alle variabili spaziali rappresentano le componenti della velocità del fluido)

$Y(t)$: dipendenza temporale della differenza di temperatura tra la parte ascendente e quella discendente del fluido

$Z(t)$: dipendenza temporale della deviazione dalla linearità della temperatura in funzione della posizione verticale



Celle convettive di Rayleigh-Bénard

generate dalla differenza di temperatura tra la superficie inferiore e quella superiore del recipiente contenente il fluido (see also <https://www.youtube.com/watch?v=gSTNxS96fRg>)

The Lorenz Equations

The Lorenz model is based on a (gross) simplification of the fundamental Navier-Stokes equations for fluids. As shown in Appendix C, the fluid motion and resulting temperature differences can be expressed in terms of three variables, conventionally called $X(t)$, $Y(t)$, and $Z(t)$.



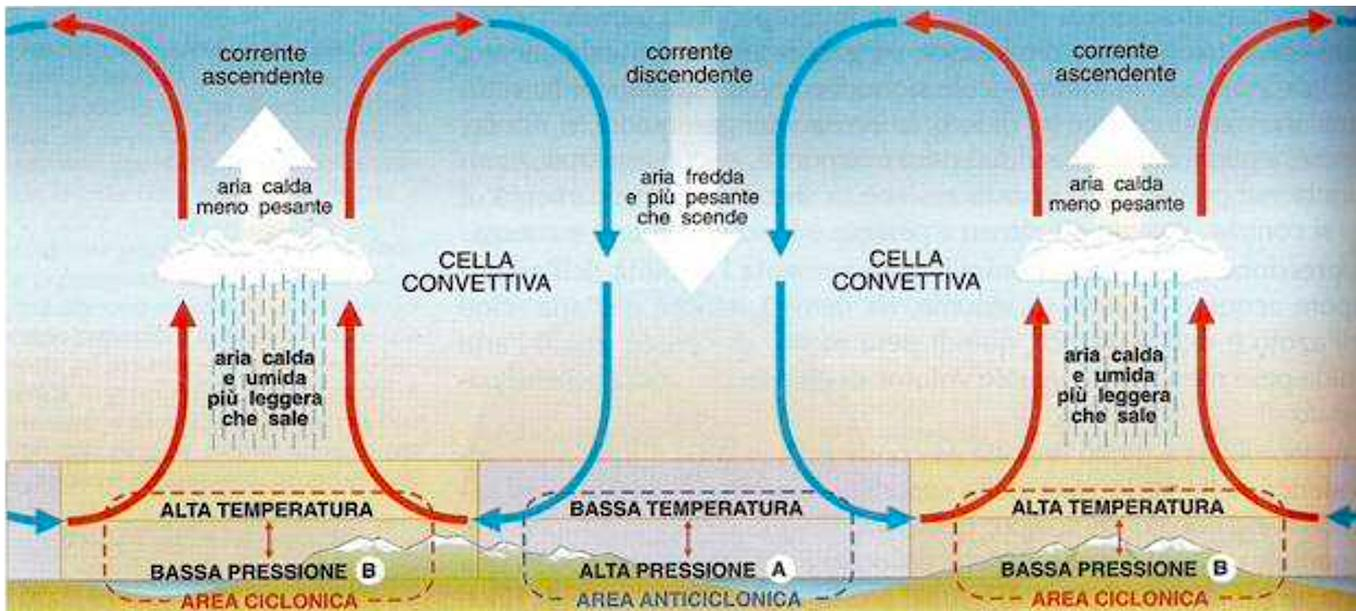
$$\begin{cases} \dot{X} = p(Y - X) \\ \dot{Y} = -XZ + rX - Y \\ \dot{Z} = XY - bZ \end{cases}$$

Significato delle 3 variabili:

$X(t)$: dipendenza temporale della funzione di flusso del fluido (le cui derivate rispetto alle variabili spaziali rappresentano le componenti della velocità del fluido)

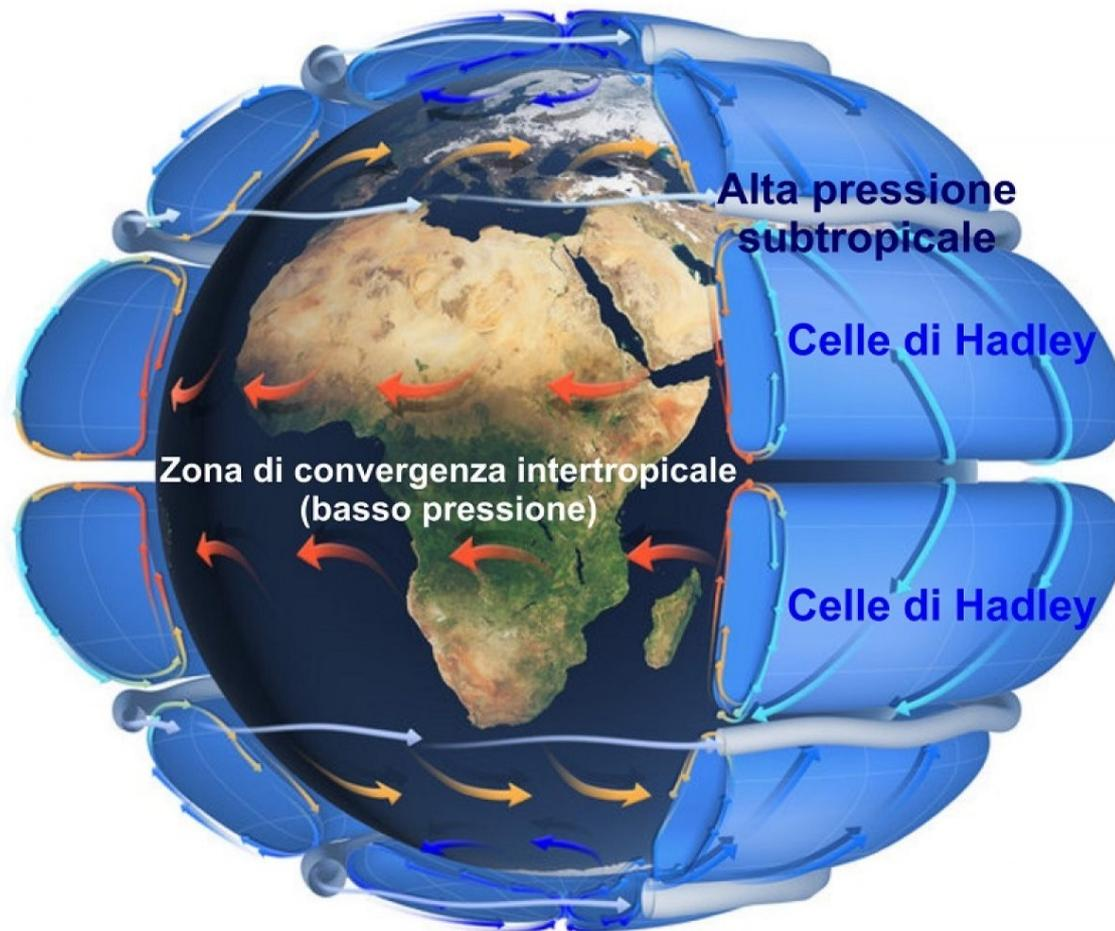
$Y(t)$: dipendenza temporale della differenza di temperatura tra la parte ascendente e quella discendente del fluido

$Z(t)$: dipendenza temporale della deviazione dalla linearità della temperatura in funzione della posizione verticale



The Lorenz Equations

The Lorenz model is based on a (gross) simplification of the fundamental Navier-Stokes equations for fluids. As shown in Appendix C, the fluid motion and resulting temperature differences can be expressed in terms of three variables, conventionally called $X(t)$, $Y(t)$, and $Z(t)$.

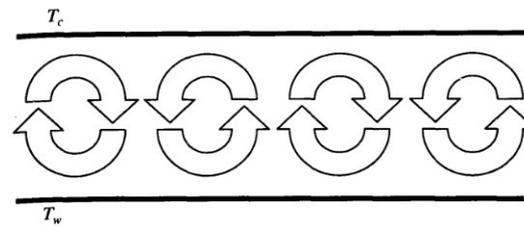
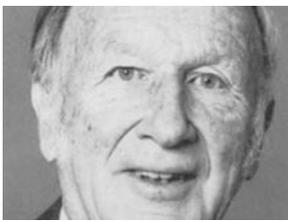


Significato delle 3 variabili:

$X(t)$: dipendenza temporale della funzione di flusso del fluido (le cui derivate rispetto alle variabili spaziali rappresentano le componenti della velocità del fluido)

$Y(t)$: dipendenza temporale della differenza di temperatura tra la parte ascendente e quella discendente del fluido

$Z(t)$: dipendenza temporale della deviazione dalla linearità della temperatura in funzione della posizione verticale



$$\begin{cases} \dot{X} = \rho(Y - X) \\ \dot{Y} = -XZ + rX - Y \\ \dot{Z} = XY - bZ \end{cases}$$

Significato dei 3 parametri di controllo:

Prandtl number ρ :
rapporto tra la viscosità cinetica del fluido e il coefficiente di diffusione termica

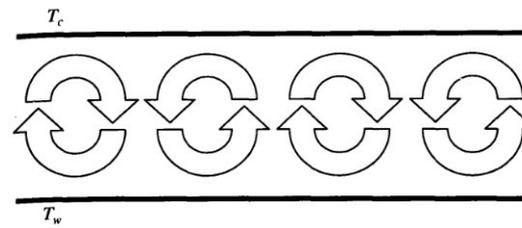
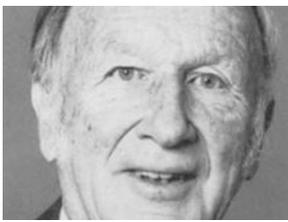
Rayleigh number r :
misura della differenza di temperatura tra la parte superiore e quella inferiore del fluido

Parameter b :
esprime il rapporto tra l'altezza verticale dello strato di fluido e la dimensione orizzontale delle celle convettive

ρ , r , and b are adjustable parameters: ρ is the so-called Prandtl number, which is defined to be the ratio of the kinetic viscosity of the fluid to its thermal diffusion coefficient. In rough terms, the Prandtl number compares the rate of energy loss from a small “packet” of fluid due to viscosity (friction) to the rate of energy loss from the packet due to thermal conduction. r is proportional to the Rayleigh number, which is a dimensionless measure of the temperature difference between the bottom and top of the fluid layer. As the temperature difference increases, the Rayleigh number increases. The final parameter b is related to the ratio of the vertical height h of the fluid layer to the horizontal size of the convection rolls. It turns out that for $b = 8/3$, the convection begins for the smallest value of the Rayleigh number, that is, for the smallest value of the temperature difference δT .

This is the value usually chosen for the study of the Lorenz model. ρ is then chosen for the particular fluid under study. Lorenz (LOR63) used the value $\rho = 10$ (which corresponds roughly to cold water), a value that had been used in a previous study of Rayleigh–Bénard convection by Saltzman (SAL62). We let r , the Rayleigh number, be the adjustable control parameter.

The Lorenz model, although based on what appears to be a very simple set of differential equations, exhibits very complex behavior. The equations look so simple that one is led to guess that it would be easy to write down their solutions, that is, to give X , Y , and Z as functions of time. In fact, as we shall discuss later, it is now believed that it is in principle impossible to give the solutions in analytic form, that is, to write down a formula that would give X , Y , and Z for any instant of time. Thus, we must solve the equations numerically, which, in practice, means that a computer does the numerical integration for us. Here, we will describe just a few results of such an integration. The analytic underpinnings for these results will be discussed later.



$$\begin{cases} \dot{X} = \rho(Y - X) \\ \dot{Y} = -XZ + rX - Y \\ \dot{Z} = XY - bZ \end{cases}$$

Significato dei 3 parametri di controllo:

Prandtl number ρ :
rapporto tra la viscosità cinetica del fluido e il coefficiente di diffusione termica

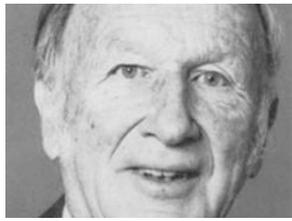
Rayleigh number r :
misura della differenza di temperatura tra la parte superiore e quella inferiore del fluido

Parameter b :
esprime il rapporto tra l'altezza verticale dello strato di fluido e la dimensione orizzontale delle celle convettive

ρ , r , and b are adjustable parameters: ρ is the so-called Prandtl number, which is defined to be the ratio of the kinetic viscosity of the fluid to its thermal diffusion coefficient. In rough terms, the Prandtl number compares the rate of energy loss from a small “packet” of fluid due to viscosity (friction) to the rate of energy loss from the packet due to thermal conduction. r is proportional to the Rayleigh number, which is a dimensionless measure of the temperature difference between the bottom and top of the fluid layer. As the temperature difference increases, the Rayleigh number increases. The final parameter b is related to the ratio of the vertical height h of the fluid layer to the horizontal size of the convection rolls. It turns out that for $b = 8/3$, the convection begins for the smallest value of the Rayleigh number, that is, for the smallest value of the temperature difference δT .

This is the value usually chosen for the study of the Lorenz model. ρ is then chosen for the particular fluid under study. Lorenz (LOR63) used the value $\rho = 10$ (which corresponds roughly to cold water), a value that had been used in a previous study of Rayleigh–Bénard convection by Saltzman (SAL62). We let r , the Rayleigh number, be the adjustable control parameter.

The Lorenz model, although based on what appears to be a very simple set of differential equations, exhibits very complex behavior. The equations look so simple that one is led to guess that it would be easy to write down their solutions, that is, to give X , Y , and Z as functions of time. In fact, as we shall discuss later, it is now believed that it is in principle impossible to give the solutions in analytic form, that is, to write down a formula that would give X , Y , and Z for any instant of time. Thus, we must solve the equations numerically, which, in practice, means that a computer does the numerical integration for us. Here, we will describe just a few results of such an integration. The analytic underpinnings for these results will be discussed later.



Behavior of Solutions to the Lorenz Equations

For small values of the parameter r , that is, for small temperature differences δT , the model predicts that the stationary, nonconvecting state is the stable condition. In terms of the variables X , Y , and Z , this state is described by the values $X = 0$, $Y = 0$, and $Z = 0$. For values of r just greater than 1, steady convection sets in. There are two possible convective states: one corresponding to clockwise rotation, the other to counterclockwise for a given convective roll. As we shall see, some initial conditions lead to one state, other conditions to the other state. Lord Rayleigh showed that if $p > b + 1$, then this steady convection is unstable for large enough r and gives way to more complex behavior. As r increases, the behavior has regions of chaotic behavior intermixed with regions of periodicity and regions of "intermittency," which cycle back and forth, apparently randomly, between chaotic and periodic behavior.

$r < 1$

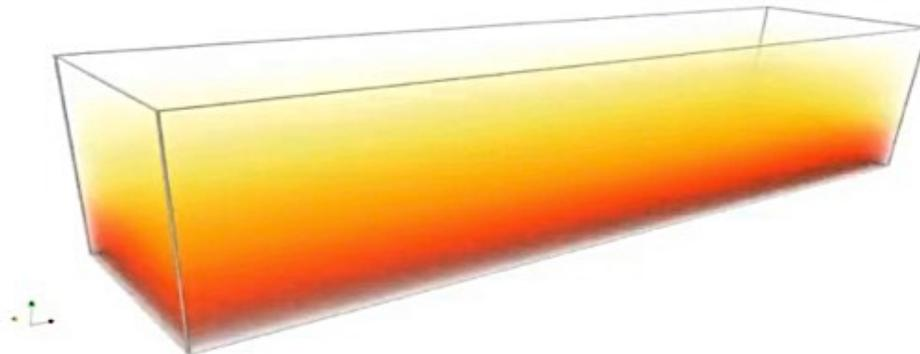
$r > 1$

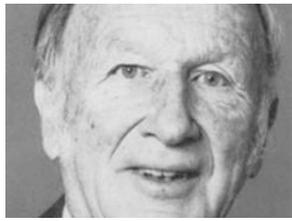
$$\begin{cases} \dot{X} = p(Y - X) \\ \dot{Y} = -XZ + rX - Y \\ \dot{Z} = XY - bZ \end{cases}$$

$p=10, b=8/3$

$r < 1$

To illustrate some of this behavior, let us start our examination of the Lorenz model by looking at the behavior of the system for values of r less than 1. Rayleigh's analysis predicts that the system should settle into the steady, nonconvective state indicated by $X = 0, Y = 0, Z = 0$. Figure 1.17 shows the results of a numerical integration of the Lorenz equations starting from the initial state $X = 0, Y = 1, Z = 0$; that is, we have started the system with a small amount of circulation and slight temperature deviations. As time goes on, however, the system relaxes to the steady nonconvective state at $X = 0, Y = 0, Z = 0$.





Behavior of Solutions to the Lorenz Equations

For small values of the parameter r , that is, for small temperature differences δT , the model predicts that the stationary, nonconvecting state is the stable condition. In terms of the variables X , Y , and Z , this state is described by the values $X = 0$, $Y = 0$, and $Z = 0$. For values of r just greater than 1, steady convection sets in. There are two possible convective states: one corresponding to clockwise rotation, the other to counterclockwise for a given convective roll. As we shall see, some initial conditions lead to one state, other conditions to the other state. Lord Rayleigh showed that if $p > b + 1$, then this steady convection is unstable for large enough r and gives way to more complex behavior. As r increases, the behavior has regions of chaotic behavior intermixed with regions of periodicity and regions of “intermittency,” which cycle back and forth, apparently randomly, between chaotic and periodic behavior.

$r < 1$

$$\dot{X} = p(Y - X)$$

$$\dot{Y} = -XZ + rX - Y$$

$$\dot{Z} = XY - bZ$$

$$p=10, b=8/3$$

 **WolframAlpha**

$\{\{10(y-x)\},\{-xz+rx-y\},\{xy-(8/3)z\}\}$

Real root

$$x = 0, \quad y = 0, \quad z = 0$$

Roots

$$x = -2\sqrt{\frac{2}{3}}\sqrt{r-1}, \quad y = -2\sqrt{\frac{2}{3}}\sqrt{r-1}, \quad z = r-1$$

$$x = 2\sqrt{\frac{2}{3}}\sqrt{r-1}, \quad y = 2\sqrt{\frac{2}{3}}\sqrt{r-1}, \quad z = r-1$$

PUNTI FISSI:

4.5 Fixed Points in Three Dimensions (dim = 0)

The fixed points of the system of Eqs. (4.4-1) are found, of course, by setting the three time derivatives equal to 0. [Two-dimensional forced systems, even if written in the three-dimensional form (4.4-4), do not have any fixed points because, as the last of Eqs. (4.4-4) shows, we never have $\dot{x}_3 = t = 0$. Thus, we will need other techniques to deal with them.] The nature of each of the fixed points is determined by the three characteristic values of the Jacobian matrix of partial derivatives evaluated at the fixed point in question. The Jacobian matrix is

$$J = \begin{pmatrix} \frac{\partial f_1}{\partial x_1} & \frac{\partial f_1}{\partial x_2} & \frac{\partial f_1}{\partial x_3} \\ \frac{\partial f_2}{\partial x_1} & \frac{\partial f_2}{\partial x_2} & \frac{\partial f_2}{\partial x_3} \\ \frac{\partial f_3}{\partial x_1} & \frac{\partial f_3}{\partial x_2} & \frac{\partial f_3}{\partial x_3} \end{pmatrix} \quad (4.5-1)$$

In finding the characteristic values of this matrix, we will generally have a cubic equation, whose roots will be the three characteristic values labeled $\lambda_1, \lambda_2, \lambda_3$.

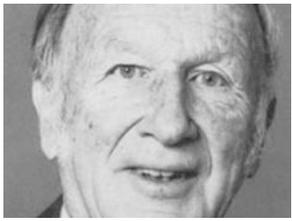
4.5 Fixed Points in Three Dimensions (dim = 0)

The fixed points of the system of Eqs. (4.4-1) are found, of course, by setting the three time derivatives equal to 0. [Two-dimensional forced systems, even if written in the three-dimensional form (4.4-4), do not have any fixed points because, as the last of Eqs. (4.4-4) shows, we never have $\dot{x}_3 = t = 0$. Thus, we will need other techniques to deal with them.] The nature of each of the fixed points is determined by the three characteristic values of the Jacobian matrix of partial derivatives evaluated at the fixed point in question. The Jacobian matrix is

Jacobiano del
modello di Lorenz,
da calcolare in
corrispondenza di
ciascun punto fisso

$$J = \begin{pmatrix} -p & p & 0 \\ r - Z & -1 & -X \\ Y & X & -b \end{pmatrix} \quad (4.5-1)$$

In finding the characteristic values of this matrix, we will generally have a cubic equation, whose roots will be the three characteristic values labeled $\lambda_1, \lambda_2, \lambda_3$.



$\{-p,p,0\},\{(r-z),-1,-x\},\{y,x,-b\}$ where $p=10,b=8/3,r=0.5,x=0,y=0,z=0$



Examples Random

$r = 0.5$

STUDIO DELLA STABILITA' DEL PUNTO FISSO:

$X=0$

$Y=0$

$Z=0$

(UNICO PUNTO FISSO PER $0 < r < 1$)

Input interpretation:

$$\begin{pmatrix} -p & p & 0 \\ r-z & -1 & -x \\ y & x & -b \end{pmatrix} \text{ where } p = 10, b = \frac{8}{3}, r = 0.5, x = 0, y = 0, z = 0$$

Result:

$$\{-10, 10, 0\}, \{0.5, -1, 0\}, \left\{0, 0, -\frac{8}{3}\right\}$$

Characteristic polynomial:

$$-x^3 - 13.6667x^2 - 34.3333x - 13.3333$$

Eigenvalues:

$$\lambda_1 \approx -10.5249$$

$$\lambda_2 \approx -2.66667$$

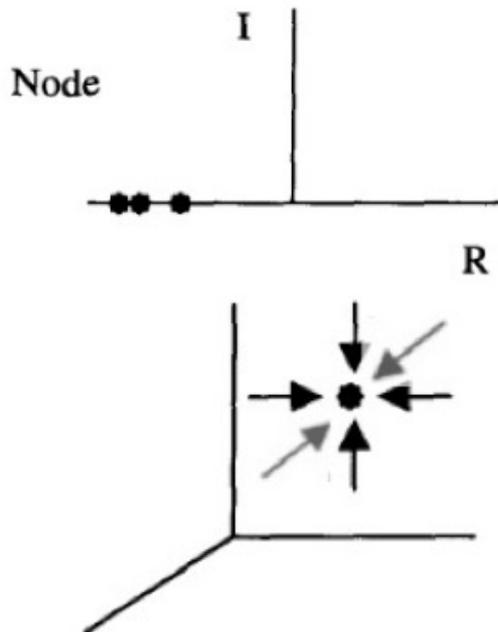
$$\lambda_3 \approx -0.475062$$

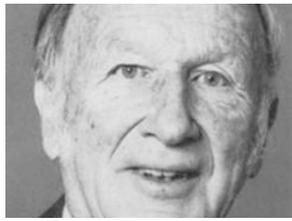
Eigenvectors:

$$v_1 \approx (-0.998625, 0.0524216, 0.)$$

$$v_2 \approx (0., 0., 1.)$$

$$v_3 \approx (-0.724097, -0.689698, 0.)$$





It will be useful to look at this behavior in two complementary graphic presentations. One graph plots the variables X , Y , and Z as functions of time, as in Fig. 1.17(a–c). The other graphs display the evolution of the system by following the motion of a point in XYZ space. Since the variables X , Y , and Z specify the state of the system for the Lorenz model, we call this space the state space for the system. For the Lorenz model, the state space is three-dimensional. We will usually follow the system with a two-dimensional projection, say on the XY or ZX planes of this state space. As time goes on, the point in state space will follow a path, which we shall call a trajectory. Figure 1.17(d) shows a ZX plane projection of the trajectory in state space. From Fig. 1.17, we see that the trajectory “relaxes” to the condition $X = 0$, $Y = 0$, and $Z = 0$ corresponding to the nonconvecting state illustrated in Fig. 1.15.

$$\begin{cases} \dot{X} = p(Y - X) \\ \dot{Y} = -XZ + rX - Y \\ \dot{Z} = XY - bZ \end{cases}$$

$$p=10, b=8/3$$

$$r = 0.5$$

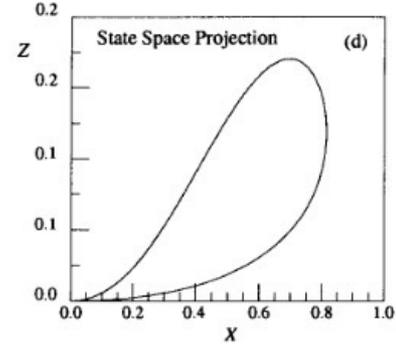
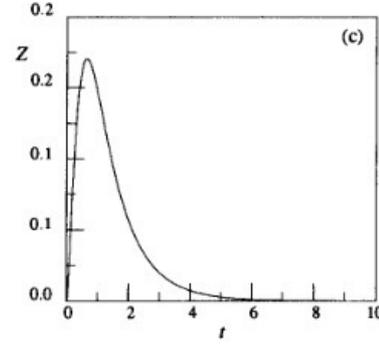
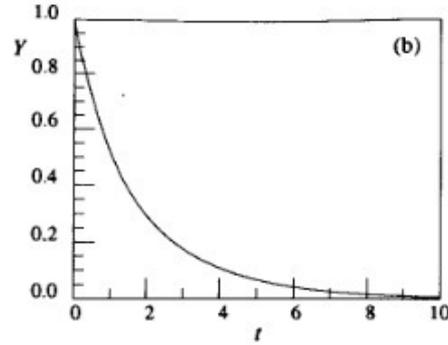
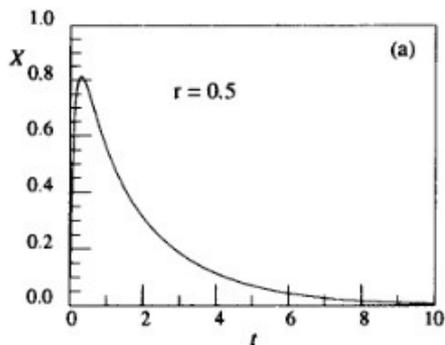
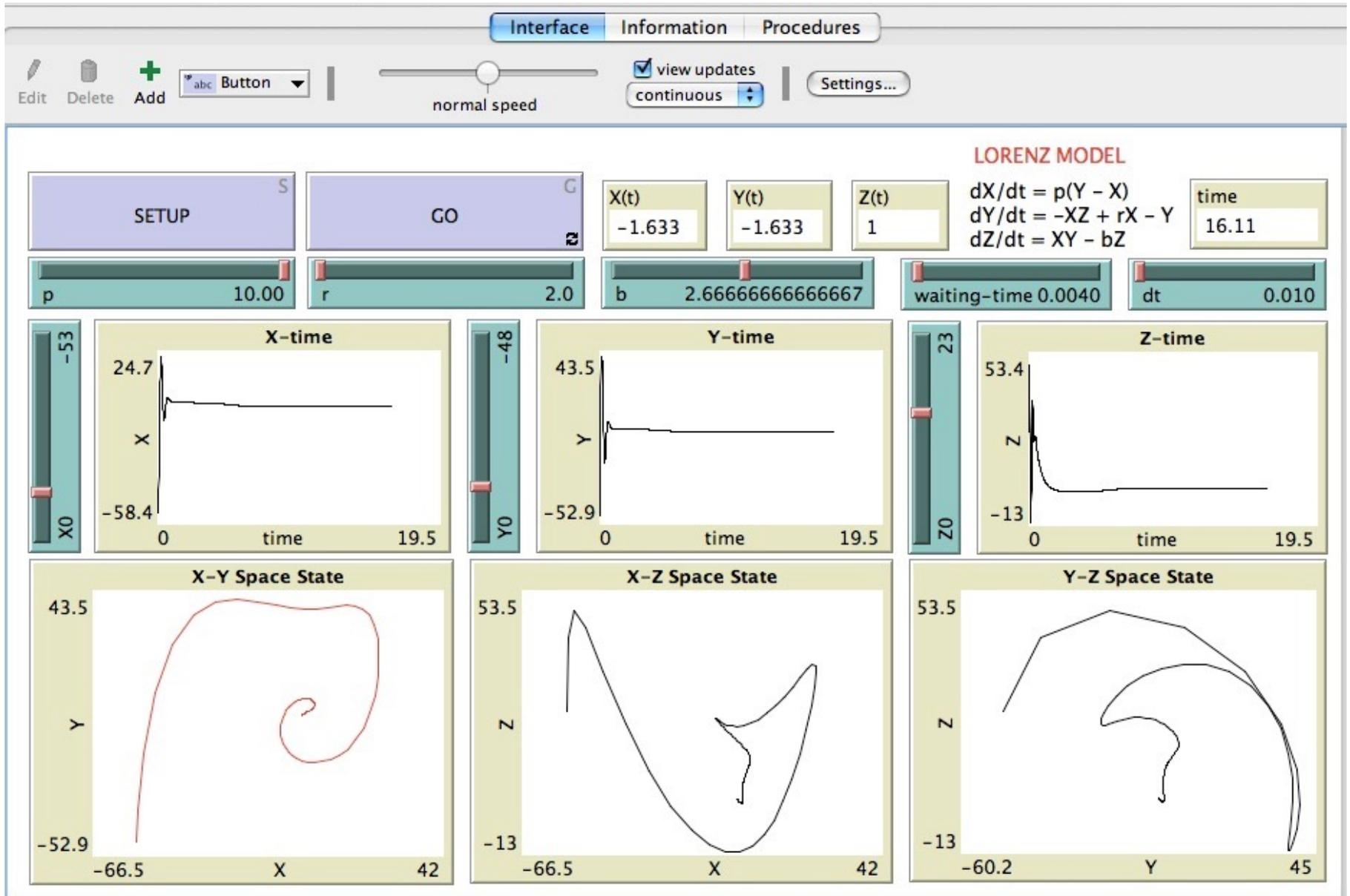
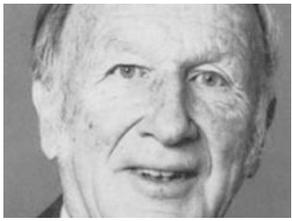


Fig. 1.17. In (a), (b), and (c), X , Y , and Z are plotted as functions of time for the Lorenz model with $r = 0.5$, $p = 10$, and $b = 8/3$. In (d), the trajectory is shown as a projection onto the ZX plane of state space. In all cases the trajectory started at the initial point $X = 0$, $Y = 1$, $Z = 0$.

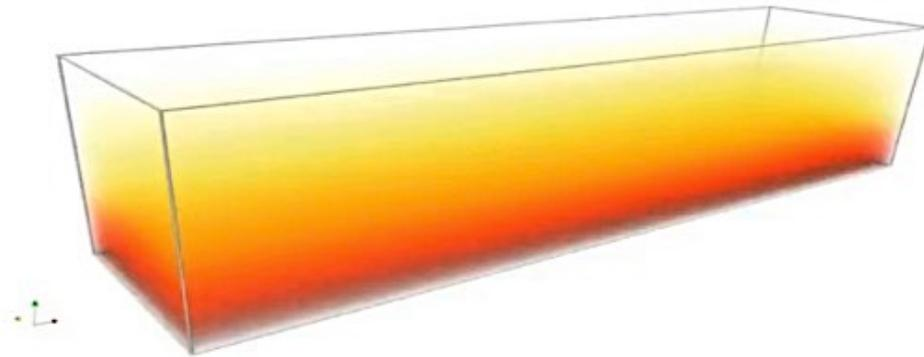
lorenz-model.nlogo





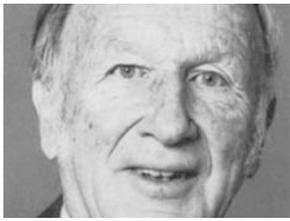
$$\begin{cases} \dot{X} = p(Y - X) \\ \dot{Y} = -XZ + rX - Y \\ \dot{Z} = XY - bZ \end{cases}$$

$$p=10, b=8/3$$



RIEPILOGO PARZIALE:

- $r < 1$: un unico **nodo** nell'origine.



For r values less than 1, all trajectories, no matter what their initial conditions, eventually end up approaching the fixed point at the origin of our XYZ state space. To use the language introduced for the logistic map, we can say that for $r < 1$, all of the XYZ space is the *basin of attraction* for the *attractor* at the origin.

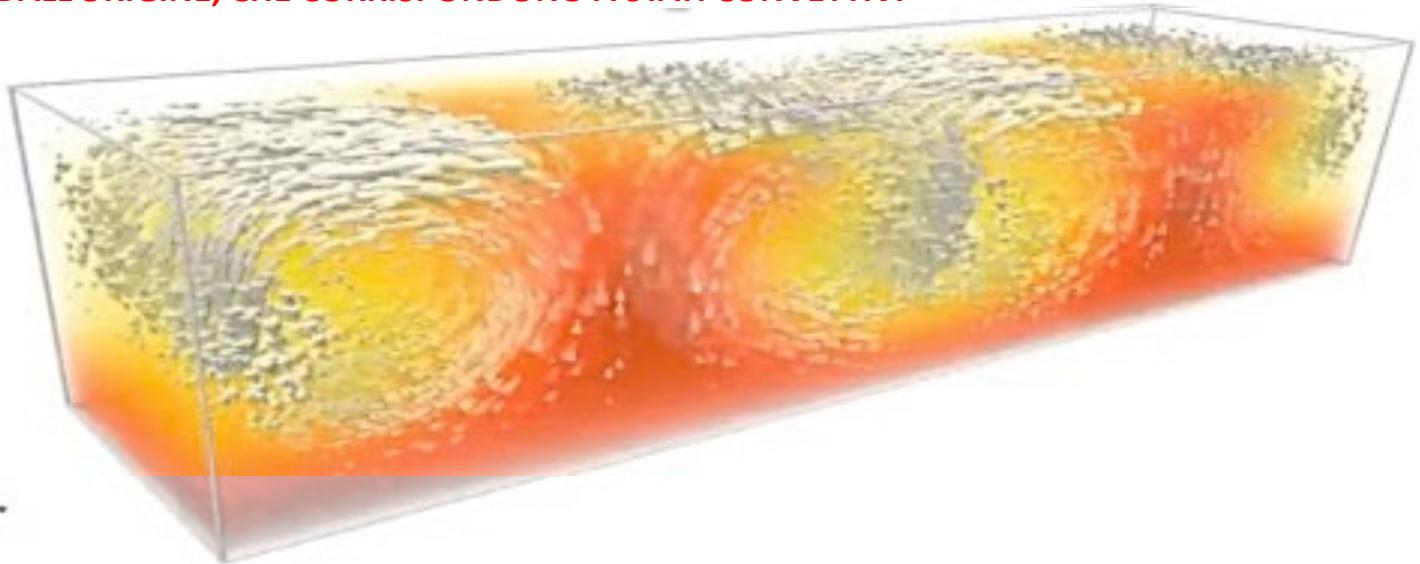
For $r > 1$, we have three fixed points. The one at the origin turns out to be a repelling fixed point in the sense that trajectories starting near it tend to move away from it. The other two fixed points are attracting fixed points if r is not too large. Some initial conditions give rise to trajectories that approach one of the fixed points; other initial conditions give rise to trajectories that approach the other fixed point. (In Chapter 4, we will see more quantitatively what is different about these fixed points.) For r just greater than 1, the other two fixed points become the attractors in the state space. Thus, we say that $r = 1$ is a bifurcation point for the Lorenz model.

$$\begin{cases} \dot{X} = p(Y - X) \\ \dot{Y} = -XZ + rX - Y \\ \dot{Z} = XY - bZ \end{cases}$$

$$p=10, b=8/3$$

$$r > 1$$

**NASCONO GLI ALTRI DUE PUNTI FISSI REALI FUORI
DALL'ORIGINE, CHE CORRISPONDONO A STATI CONVETTIVI**



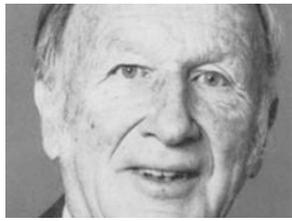


Figure 1.18 illustrates the behavior of two trajectories starting from different initial points.

Let us describe this behavior in more physical terms. If r increases to a value just greater than 1 (recall that this means that we have increased the temperature difference between the bottom and top of the fluid layer), the fixed point at the origin becomes a repelling fixed point. This tells us that the so-called conductive state (the state with no fluid convection) has become unstable. The slightest deviation from the conditions $X = 0, Y = 0, Z = 0$ sends the state space trajectory away from the origin. For r just greater than 1, the trajectories are attracted to one or the other of the other two fixed points at $X = Y = \pm\sqrt{b(r-1)}$. Those two fixed points correspond to steady (time-independent) convection, one with clockwise rotation, the other counterclockwise. Some initial conditions give rise to trajectories that head toward one fixed point; other initial conditions lead to the other fixed point. The left-hand side of Fig. 1.18 shows the YZ plane state space projection for a trajectory starting from $X = 0, Y = -1, Z = 0$. The right-hand side of Fig. 1.18 shows a trajectory starting from a different set of initial values: $X = 0, Y = +1, Z = 0$. Note, in particular, that the system settles into a state with nonzero values of Y and Z , that is, the fluid is circulating.

$$\begin{cases} \dot{X} = p(Y - X) \\ \dot{Y} = -XZ + rX - Y \\ \dot{Z} = XY - bZ \end{cases}$$

$$p=10, b=8/3$$

$$r = 2$$

$$X = Y = \pm\sqrt{8/3} = \pm 1.63\dots$$

 WolframAlpha

`{{10(y-x)},{-xz+2x-y},{xy-(8/3)z}}`

Roots:

$$\begin{aligned} &x = 0, \quad y = 0, \quad z = 0 \\ &x = -2\sqrt{\frac{2}{3}}, \quad y = -2\sqrt{\frac{2}{3}}, \quad z = 1 \\ &x = 2\sqrt{\frac{2}{3}}, \quad y = 2\sqrt{\frac{2}{3}}, \quad z = 1 \end{aligned}$$

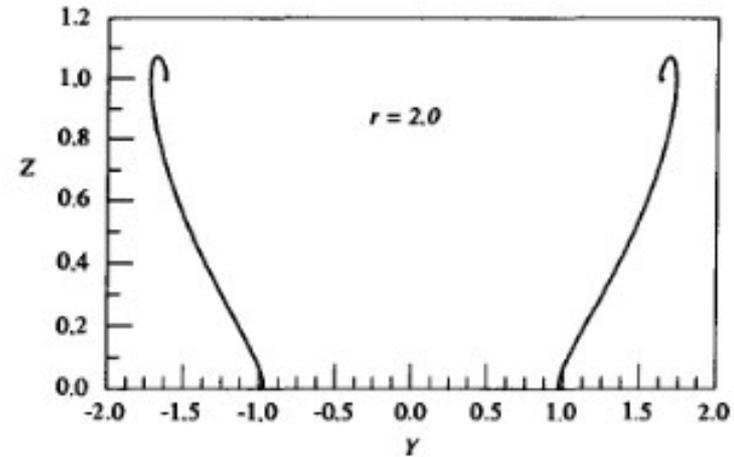
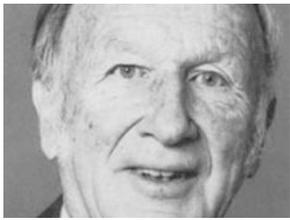


Fig. 1.18. State space projections onto the YZ plane for trajectories in the Lorenz model with $r = 2$. One attractor corresponds to clockwise rotation, the other to counterclockwise rotation of the fluid at a particular spatial location.

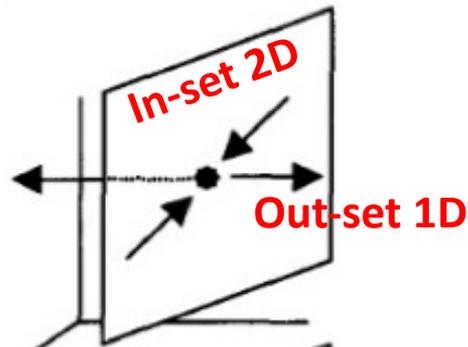
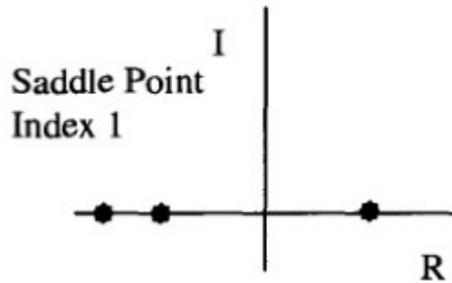


STUDIO DELLA STABILITA' DEL PUNTO FISSO:

$$X=0$$

$$Y=0$$

$$Z=0$$



$\{\{-p,p,0\},\{(r-z),r,-x\},\{y,x,-b\}\}$ where $p=10,b=8/3,r=2,x=0,y=0,z=0$



$r = 2$

Examples Random

Input Interpretation:

$$\begin{pmatrix} -p & p & 0 \\ r-z & -1 & -x \\ y & x & -b \end{pmatrix} \text{ where } p = 10, b = \frac{8}{3}, r = 2, x = 0, y = 0, z = 0$$

Result:

$$\{\{-10, 10, 0\}, \{2, -1, 0\}, \{0, 0, -\frac{8}{3}\}\}$$

Characteristic polynomial:

$$-x^3 - \frac{41x^2}{3} - \frac{58x}{3} + \frac{80}{3}$$

Eigenvalues:

Exact forms

$$\lambda_1 \approx -11.8443$$

$$\lambda_2 \approx -2.66667$$

$$\lambda_3 \approx 0.844289$$

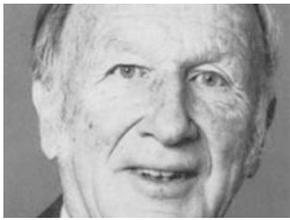
Eigenvectors:

Exact forms

$$v_1 \approx (-5.42214, 1., 0.)$$

$$v_2 \approx (0., 0., 1.)$$

$$v_3 \approx (0.922144, 1., 0.)$$

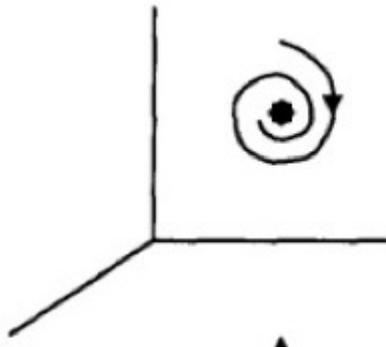
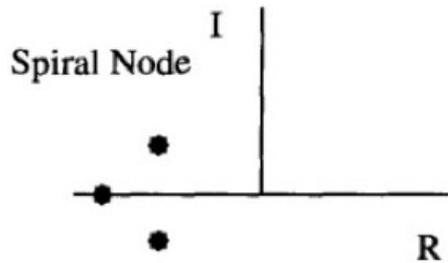


STUDIO DELLA STABILITA' DEL PUNTO FISSO:

$$X = -1.63...$$

$$Y = -1.63...$$

$$Z = 1$$



$\{\{-p,p,0\},\{(r-z),-1,-x\},\{y,x,-b\}\}$ where $p=10,b=8/3,r=2,x=-1.63,y=-1.63,z=1$



Examples Random

$$r = 2$$

Input Interpretation:

$$\begin{pmatrix} -p & p & 0 \\ r-z & -1 & -x \\ y & x & -b \end{pmatrix} \text{ where } p = 10, b = \frac{8}{3}, r = 2, x = -1.63, y = -1.63, z = 1$$

Result:

$$\{-10, 10, 0\}, \{1, -1, 1.63\}, \left\{-1.63, -1.63, -\frac{8}{3}\right\}$$

Characteristic polynomial:

$$-x^3 - 13.6667x^2 - 31.9902x - 53.138$$

Eigenvalues:

$$\lambda_1 \approx -11.2414$$

$$\lambda_2 \approx -1.21263 + 1.80458 i$$

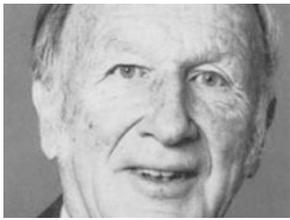
$$\lambda_3 \approx -1.21263 - 1.80458 i$$

Eigenvectors:

$$v_1 \approx (0.979108, -0.121548, 0.163016)$$

$$v_2 \approx (-0.370106 - 0.378644 i, -0.256897 - 0.399518 i, 0.702879 + 0. i)$$

$$v_3 \approx (-0.370106 + 0.378644 i, -0.256897 + 0.399518 i, 0.702879 + 0. i)$$

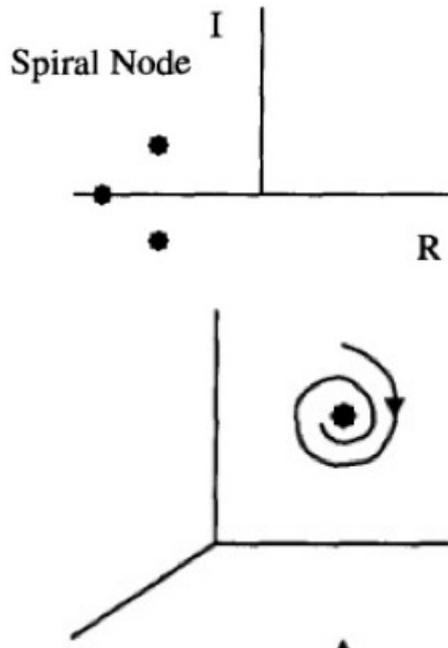


STUDIO DELLA STABILITA' DEL PUNTO FISSO:

$$X=1.63\dots$$

$$Y=1.63\dots$$

$$Z=1$$



$\{-p,p,0\},\{r-z,-1,-x\},\{y,x,-b\}$ where $p=10,b=8/3,r=2,x=1.63,y=1.63,z=1$



Examples Random

$$r = 2$$

Input interpretation:

$$\begin{pmatrix} -p & p & 0 \\ r-z & -1 & -x \\ y & x & -b \end{pmatrix} \text{ where } p = 10, b = \frac{8}{3}, r = 2, x = 1.63, y = 1.63, z = 1$$

Result:

$$\{-10, 10, 0\}, \{1, -1, -1.63\}, \left\{1.63, 1.63, -\frac{8}{3}\right\}$$

Characteristic polynomial:

$$-x^3 - 13.6667x^2 - 31.9902x - 53.138$$

Eigenvalues:

$$\lambda_1 \approx -11.2414$$

$$\lambda_2 \approx -1.21263 + 1.80458 i$$

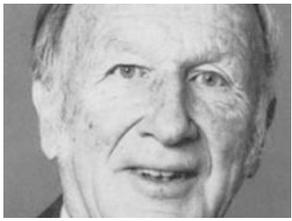
$$\lambda_3 \approx -1.21263 - 1.80458 i$$

Eigenvectors:

$$v_1 \approx (0.979108, -0.121548, -0.163016)$$

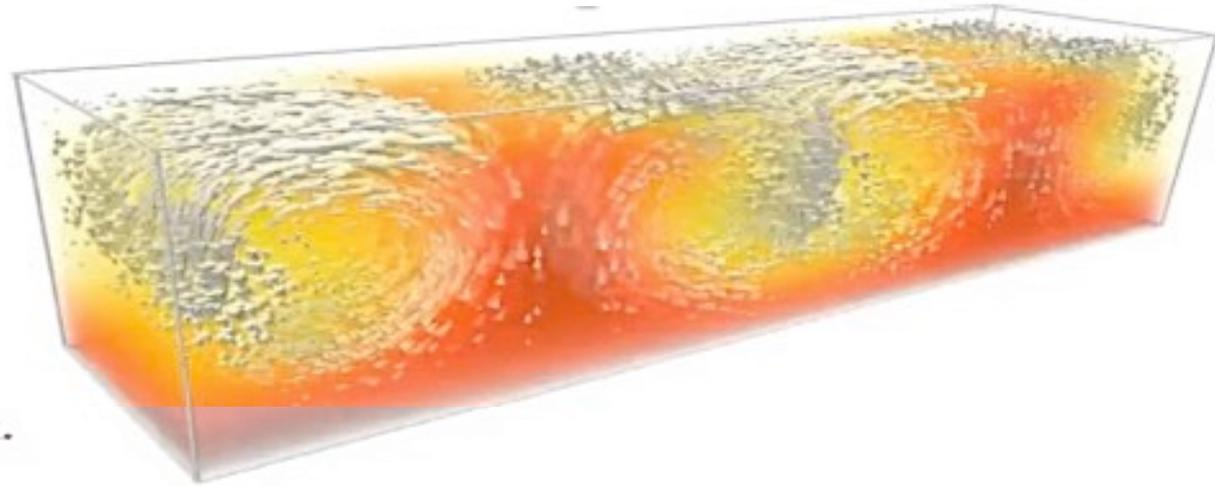
$$v_2 \approx (-0.370106 - 0.378644 i, -0.256897 - 0.399518 i, -0.702879 + 0. i)$$

$$v_3 \approx (-0.370106 + 0.378644 i, -0.256897 + 0.399518 i, -0.702879 + 0. i)$$



$$\begin{cases} \dot{X} = p(Y - X) \\ \dot{Y} = -XZ + rX - Y \\ \dot{Z} = XY - bZ \end{cases}$$

$$p=10, b=8/3$$



RIEPILOGO PARZIALE:

- $r < 1$: un unico **nodo** nell'origine.
- $1 < r < 13.93$: un **saddle point** (index 1) nell'origine + due **nodi a spirale** simmetrici off-origine.

Cosa succede per $r > 13.93$?